DESIGN AND CONTROL OF FIXED-BEDS AFFECTED BY CATALYST DEACTIVATION

By

Jan-Chen Hong

A DISSERTATION PRESENTED TO THE GRADUATE COUNCIL OF THE UNIVERSITY OF FLORIDA IN PARTIAL FULFILLMENT OF THE REQUIREMENTS FOR THE DEGREE OF DOCTOR OF PHILOSOPHY

UNIVERSITY OF FLORIDA

1984

ACKNOWLEDGMENTS

The author wishes to express his sincere appreciation to his research advisor, Dr. Hong H. Lee, for his guidance, patience, and constant encouragement throughout this work. Particular thanks are also due to Drs. G.B. Hoflund, C.C. Hsu, J.P. O'Connell and S. Svoronos for serving on the advisory committee.

The author also wishes to express his gratitude to his colleagues Laks Akella, Irfan Toor and Karen Klingman for many stimulating discussions, to staff members Tracy Lambert and Ron Baxley for their assistance in fabricating the experimental apparatus, and to Derbra Owete for typing the manuscript.

Sincere appreciation is extended to his parents, Mr. and Mrs. I-Mo Hong and to his wife, Shiao-Ing for their support and understanding throughout his graduate study.

TABLE OF CONTENTS

NOTATION

A_i, A_D	preexponential factor, i=1, 2, q
a_1	$-\Delta H_2/\rho C_p$
a_2	$-\Delta H_1(1-\Delta H_2/\Delta H_1)/\rho C_p b_1$
a_3	$(-\Delta H_1 - b\Delta H_2)/\rho C_p$
a_4	$-\Delta H_2/\rho C_p$
b_1, b_2	ratios of stoichiometric coefficients
C	concentration of main reactant; integration constant
C_d	desired outlet concentration of main reactant
$\tilde{C}_d$	modified C_d given by Eq. (2-16)
C_{d_o}	initial value of C_d
C_{in}	inlet concentration of main reactant
C_p	specific heat of reaction fluid
$(C_p)_c$	specific heat of coolant
D_e	effective diffusivity
E_a, E_i	activation energy for main reaction i=1, 2, q
E_D	activation energy for deactivation reaction
F	molar flow rate
F_o	molar flow rate of reactant mixture at the inlet
f	apparent concentration dependence of rate of main reaction; temperature and activity dependence of X in Eq. (4-2)

G_i	E_i/R_g, i = 1,2,q,D
g	concentration dependence of intrinsic rate of reaction; temperature and activity dependence of rate of deactivation in Eq. (4-1)
H	reactor activity factor defined by Eq. (2-7)
H_c	current value of H
H_n	new value of H
$(-\Delta H)$	heat of reaction
h	local activity factor defined by Eq. (2-5)
h_c	current value of h
h_f	h at $t = t_f$
h_m	film heat transfer coefficient
h_n	new value of h
I	integral defined by Eq. (2-20)
J	performance index
K_D	rate constant for deactivation reaction
K_1	$k_1 k_q$
K_2	$k_2 k_q$
K_j	equilibrium constant
K_q	$P_{Ao}\, k_q$
k	intrinsic rate constant
k_q	adsorption equilibrium constant
k_a	apparent rate constant
k_{a_o}	preexponential factor for k_a
k_{p_s}	rate constant for poisoning reaction evaluated at pellet surface temperature

m	mass rate of reaction fluid; order of deactivation reaction
m_c	mass rate of coolant
N	concentration of poisoning species
n	number of control steps in piecewise control
P	total pressure
P_A	partial pressure for species A
p_i	E_i/E_D, i=1,2,q
Q	deactivation capacity of catalyst
q	quantity defined by Eq. (2-21)
R_g	gas constant
R_G	global rate of main reaction
R_t	tube radius
r	intrinsic rate
S	selectivity
T	temperature of reaction fluid
$\bar{T}$	transformed function of T
T_c	coolant temperature
T_{in}	reactor inlet temperature
T_{ce}	T_c at z=0
t	time
t_f	time at which catalyst is regenerated or replaced in continuous control
t_n	time at which catalyst is regenerated or replaced in piecewise control
U	overall heat transfer coefficient

v	superficial velocity
W	weight of catalyst
X	conversion at the outlet
ΔX	bandwidth of conversion allowed before an adjustment in T_{in} is made
x	conversion in the reactor
Y	yield at the outlet
y	yield in the reactor
y'_{Ao}	mole fraction of A at the outlet
y'_{Al}	mole fraction of A at the outlet
y'_{Cl}	mole fraction of C at the outlet
Z	reactor length
z	axial reactor coordinate

Greek Letters

α	proportionality constant defined in Eq. (2-16)
α_j	$A_j/A_D^{p_j}$ $j=1,2,q$
β	h_2/h_1
γ	fraction of catalyst deactivated
ε_B	bed porosity
μ	cost incurred due to the reactor shut-down
ρ	reaction fluid density
τ	holding time given in Eq. (2-1)

Subscripts

A	species A; ethylene
B	species B; ethylene oxide
C	species C; carbon dioxide

c	coolant; current value; with constant-conversion constraint
D	deactivated
d	desired
e	reactor outlet
i	index for a step change in inlet temperature
in	inlet
max	the maximum value
min	the minimum value
n	new value
o	at t=0 or z=0
q	adsorption equilibrium constant
r	at reference state
1	reaction path 1
2	reaction path 2

Superscripts

*	optimal value
·	$\frac{d}{dt}$
~	normalized value

Abstract of Dissertation Presented to the Graduate Council of the University of Florida in Partial Fulfillment of the Requirements for the Degree of Doctor of Philosophy

DESIGN AND CONTROL OF FIXED-BEDS AFFECTED BY CATALYST DEACTIVATION

By

Jan-Chen Hong

August 1984

Chairman: Dr. H. H. Lee
Major Department: Chemical Engineering

On-line measurements of temperature and concentration and the global rate at any reference state of catalyst can be used to estimate a measure of catalyst deactivation. A feedback control policy is obtained from this measure of catalyst deactivation for manipulating the reactor outlet conversion or yield in any desired manner. This feedback control enables one to obtain the desired conversion or yield without any knowledge of deactivation kinetics, and the results are applicable to any type of deactivation. The feedback control policy has been verified by experiment based on ethylene oxidation reactions over a silver catalyst using a laboratory shell-and-tube reactor. Excellent agreements have been reached between the theory and the experiment.

The problem of finding the optimal piecewise control policy has been formulated as a multivariable optimization problem. The optimal policy is one of increasing conversion. The constant conversion policy corresponds to the limiting case where the number of piecewise steps approaches infinity. This optimal piecewise control is suitable for on-line implementation in conjunction with the on-line estimation of the extent of catalyst deactivation. An optimal continuous control policy for parallel and reversible reactions has also been solved using the technique of calculus of variations. It is shown that a direct substitution method is more efficient than the commonly used method of applying the Pontryagin maximum principle.

The optimal control policies can easily be taken into consideration for reactor design. This combination of process design and control with due consideration of catalyst deactivation for both is shown to result in a substantial improvement of the reactor performance.

CHAPTER 1

INTRODUCTION

The usual practice of operating a fixed-bed with slow catalyst deactivation is to raise the reactor inlet temperature to compensate for the declining catalytic activity so as to maintain a desired conversion (Kovarik and Butt, 1982). The catalyst is regenerated when the required temperature becomes too high. The reactor is usually designed to give the desired conversion without any consideration for the catalyst deactivation. A summary of operational strategies for a reactor subject to catalyst deactivation is listed in Table 1-1.

A number of questions can be raised regarding these usual practices: The first question is how we should control the operating conditions of a reactor designed in the usual way. This question has been the subject of many studies (Chou et al. 1967; Szepe and Levenspiel, 1968; Ogunye and Ray, 1971; Haas et al., 1974; Levenspiel and Sadana, 1978). The control policies resulting from these studies either lead to an open-loop control or require detailed knowledge of catalyst deactivation. Although considerable progress has been made in our understanding of catalyst deactivation, the deactivation is still the least understood of all facets involved in the quantitative description of a

Table 1-1 Summary of Operational Strategies for a Reactor Subject to Catalyst Deactivation

1. Vary reactor temperature with time to maintain a constant conversion with a constant reactor feed flow rate. A typical policy for large throughput (400 MM pounds per year) and slow deactivation rates (months to years of catalyst life).
2. Vary throughput of the reactor feed while holding the reactor temperature and conversion constant. A possible policy for medium deactivation rates (weeks to months catalyst life) and small to medium throughput (about 25 MM pounds per year) systems.
3. Allow the conversion to fall while holding the reactor feed flow rate and reactor temperature constant. Similar applications as in Item 2.
4. Maintain the fresh feed rate and reactor temperature constant and let the recycle flow increase. Similar application as in Item 2.
5. Use a combination of reactors in parallel and the policies of Items 1 or 3. Usually, with two reactors in parallel, one will be off-line for catalyst regeneration while the other is operating. A typical policy for large throughput and medium to fast deactivation rates (days to months of catalyst life).
6. Continuous catalyst regeneration while maintaining constant conversion, throughput, and reactor temperature. A typical policy for large throughput, rapid deactivation systems (hours to days of catalyst life).

Reprinted from Cat. Rev. 24, 499 (1982), by courtesy of Marcel Dekker, Inc.

fixed-bed. This uncertainty regarding the deactivation and the compounded effects of deactivation and diffusion in a fixed-bed make it quite unattractive to implement an open-loop control policy. The second question, therefore, is whether a measure of catalyst deactivation can be estimated from process measurements and, if so, how a feedback control can be realized with the measurements made. In Chapter 2 a method of determining a measure of catalyst deactivation is presented and the result then utilized for a feedback control policy. This feedback control policy is demonstrated in Chapter 3 with a simulation of a model reaction system, and is put to the test with a laboratory fixed-bed where ethylene oxidation reactions take place over a silver catalyst.

It has been shown that constant conversion policy is optimal only for a single irreversible reaction affected by concentration-independent deactivation, when the reactor is controlled continuously (Chou et al. 1967; Lee and Crowe, 1970; Crowe, 1970). Thus, the third question regarding the usual practice of maintaining constant conversion is what the optimal policy will be if the reactor is piecewise controlled (for example, the temperature is adjusted only once a day, rather than continuously), or if the reaction is complex. The solutions to this question are presented in Chapters 4 and 5.

A much more important question than the three discussed above has to do with the inherent interrelationship between process controllability and process design. It is intuitively clear that the process design dictates the controllability, for the parameters involved in describing a process contain design parameters which in turn dictate the way the process can be controlled. It is clear therefore, that the best possible performance of the process can be attained when the process design and control are combined. For the reactor under consideration, this means that the best possible performance can be attained when the catalyst deactivation is taken into consideration not only for the reactor control but also for the reactor design. The question, therefore, is what the reactor size and the feedback control should be for the best performance of the reactor. In Chapter 6, the answer to this question is presented.

CHAPTER 2

THEORY OF ON-LINE ESTIMATION OF DEACTIVATION AND CONTROL

An important problem in operating a fixed-bed with catalyst deactivation is that of finding a means of estimating the extent of catalyst deactivation from on-line measurements because of the uncertainty regarding the deactivation. The problem of controlling the conversion in any desired manner using a feedback scheme is another. These two problems are solved theoretically in this chapter, starting with a single reaction and then proceeding to multiple reactions.

§2-1 A Simple Reaction

Consider a shell-and-tube reactor in which a single reaction takes place. Assuming negligible radial gradients and pseudo steady-state, one-dimensional balance equations can be written as

$$\frac{dC}{dz} = -\tau R_G; \quad \tau = Z(1-\varepsilon_B)/v \qquad ; C\Big|_{z=o} = C_{in} \qquad (2\text{-}1)$$

$$\frac{dT}{dz} = \left(\frac{-\Delta H}{\rho C_p}\right)\tau R_G + \frac{(mC_p)_c}{mC_p}\frac{dT_c}{dz} \; ; \quad T\Big|_{z=o} = T_{in} \qquad (2\text{-}2)$$

$$\frac{dT_c}{dz} = -\frac{2U\pi R_t Z}{(mC_p)_c}(T-T_c) \qquad ; \qquad T_c\Big|_{z=1} = T_{c_{in}} \qquad (2\text{-}3)$$

where C and T are the concentration and temperature of the reactant, and T_c is the countercurrent coolant temperature. Here m and m_c are the reaction fluid and coolant mass rates, C_p and $(C_p)_c$ are the specific heat capacities for the reaction fluid and the coolant, Z is the reactor length, z is the axial reactor coordinate normalized with respect to Z, v is the superficial velocity assumed constant in the radial direction, ε_B is the bed porosity, U is the overall heat transfer coefficient, and R_t is the tube radius.

The global rate based on pellet volume, R_G, can be expressed as

$$R_G = h(z;t)k_a f(C,K_j) \tag{2-4}$$

where k_a is the apparent rate constant in the form of the Arrhenius relationship and f represents the apparent dependence of the rate on concentration and equilibrium constants K_j. In the absence of diffusion and deactivation effects, the apparent rate reduces to intrinsic rate. The activity factor h (Wheeler, 1955) is defined by

$$h(z;t) \equiv \frac{(R_G)_D}{(R_G)_r} \tag{2-5}$$

where the subscripts r and D denote reference-state and deactivated catalyst, respectively. According to the definition, h is unity for catalyst at the reference state. This activity factor decreases with time due to catalyst deactivation and thus depends on time. It should be recognized in Eq. (2-5) that the definition of h is general in that h can

depend on the concentration C and thus is applicable to concentration-dependent deactivation. Since C is a function of z at a given time, h(C;t) is a subset of h(z;t). The pseudo steady-state assumption is based on the fact that the time scale of catalyst deactivation is many orders of magnitude larger than that for the reactor to reach a steady state.

For the purpose of deriving an expression for a measure of the extent of deactivation, we rewrite Eq. (2-1) with the aid of Eq. (2-4) as

$$\frac{dC}{dz} = -\tau h(z;t) k_a f(C,K_j) \qquad (2\text{-}6)$$

Here again, one can write h as h(C;t) in place of h(z;t) for dependent deactivation. This equation can be integrated from the reactor inlet to the outlet to give

$$-\int_{C_{in}}^{C_e} \frac{dC}{\tau k_a(T) f(C,K_j)} = \int_0^1 h(z;t)dz \equiv H(t) \qquad (2\text{-}7)$$

where C_e and C_{in} are the concentrations at the outlet and the inlet, respectively, at any given time. By definition, H is unity at reference state since the activity factor h is uniform at unity throughout the reactor. The quantity H is a measure of the extent of catalyst deactivation which represents the activity for the reactor and thus may be termed "reactor activity factor." The value of H decreases as the outlet conversion decreases due to the catalyst deactivation for a given inlet temperature.

The temperature appearing in Eq. (2-7) needs to be related to concentration for the integration. Integrating Eq. (2-2) from the reactor inlet to z, we obtain

$$T = T_{in} + \left[\frac{-\Delta H}{\rho C_p}\right] (C_{in}-C) - \frac{(mC_p)_c}{mC_p}(T_{ce} - T_c) \qquad (2\text{-}8)$$

where T_{ce} is the coolant temperature at z=0 and T_{in} is the reactor inlet temperature. Consider first an adiabatic reactor for which Eq. (2-8) reduces to

$$T = T_{in} + \left[\frac{-\Delta H}{\rho C_p}\right] (C_{in} - C) \qquad (2\text{-}9)$$

Now that T is expressed in terms of C and readily measurable inlet conditions, the value of H can be calculated by simply carrying out the integration numerically with respect to C in Eq. (2-7) with the measured outlet concentration. For instance, the apparent rate constant $k_a(T)$ for an adiabatic reactor can be expressed as

$$k_a = k_{a_o} \exp\left\{\frac{-E_a/R_g}{T_{in} + \left[\frac{-\Delta H}{\rho C_p}\right] (C_{in} - C)}\right\} \qquad (2\text{-}10)$$

where k_{a_o} is the apparent preexponential factor and E_a is the apparent activation energy. The equilibrium constants K_j can be expressed in a similar manner. For a shell-and-tube reactor to which Eq. (2-8) applies, the calculation of H requires measurement of coolant temperature along the reactor length. This measurement can be used in Eq. (2-3) for the

calculation of T as a function of z. With these T and T_c, the corresponding change in C for a selected interval of Δz can be obtained from Eq. (2-8) which in turn can be used in Eq. (2-7) for the calculation of H.

An immediate use of the reactor activity factor calculable from the temperature and concentration measurements is in the manipulation of the reactor inlet temperature for the purpose of maintaining the desired conversion. Suppose that the inlet temperature is adjusted intermittently, as in the usual operation of a reactor, to compensate for the declining activity. Consider an adiabatic reactor for clarity. If we let the subscript c denote the current quantities and n the new quantities resulting from a change in the reactor inlet temperature, Eq. (2-7) can be written twice to give

$$H_c = \int_0^1 h_c(z;t)dz = -\int_{C_{in}}^{C_e} \frac{dC}{\tau k_a[T;(T_{in})_c]f(C,K_j)} \qquad (2\text{-}11)$$

$$H_n = \int_0^1 h_n(z;t)dz = -\int_{C_{in}}^{C_d} \frac{dC}{\tau k_a[T;(T_{in})_n]f(C,K_j)} \qquad (2\text{-}12)$$

where C_d is the desired concentration which will be attained by changing the current inlet temperature, $(T_{in})_c$, to the new inlet temperature, $(T_{in})_n$. As we shall soon see in the next section, the activity factors h_c and h_n depend mainly on the fraction of catalyst deactivated and slightly on the temperature difference between bulk fluid and pellet surface. If we neglect this change in the temperature difference for the time being, we can set

$$h_c(z;t) = h_n(z;t) \qquad (2\text{-}13)$$

for the purpose of calculating the new inlet temperature that yields the desired outlet concentration. The justification here is that the fraction of catalyst deactivated changes negligibly for all points along the reactor while the inlet temperature is adjusted from the current value to a new value. Note that the justification is still valid for concentration dependent deactivation, i.e. $h_c(C(z);t) = h_n(C(z);t)$. Equations (2-11) through (2-13) together with Eq. (2-10) can be used to obtain

$$-\int_{C_{in}}^{C_d} \frac{dC}{\tau k_{a_o} \exp\left[\dfrac{-E_a/R_g}{(T_{in})_n + \left(\dfrac{-\Delta H}{\rho C_p}\right)(C_{in} - C)}\right] f(C,K_j)} = H_c \qquad (2\text{-}14)$$

where H_c is the known, current reactor activity factor calculated from Eq. (2-12) just prior to the change in the inlet temperature based on the current measured outlet concentration C_e and inlet temperature $(T_{in})_c$. Equation (2-14) can now be solved for $(T_{in})_n$ by a numerical technique such as Newton's method or bisection method since the left hand side of the equation can be evaluated, given a value of $(T_{in})_n$. The value of $(T_{in})_n$ that satisfies Eq. (2-14) will yield the desired conversion and, therefore, the inlet temperature can be changed to $(T_{in})_n$ to maintain the conversion at the desired level.

The control policy of Eq. (2-14) is a piecewise algorithm for the manipulation of the inlet temperature. Therefore, it will maintain the conversion at the desired level only for a short period of time after a change in the inlet temperature and the conversion thereafter will gradually decrease with time until the inlet temperature is raised again. A bandwidth for the allowed decrease in conversion can be used to trigger the adjustment of the reactor inlet temperature. The control algorithm for a nonadiabatic reactor can be obtained in a similar manner. The equation corresponding to Eq. (2-14) is

$$-\int_{C_{in}}^{C_d} \frac{dC}{\tau k_a[T;(T_{in})_n]f(C,K_j)} = H_c \qquad (2\text{-}15)$$

This equation, however, needs to be solved in conjunction with Eqs. (2-3) and (2-10) for $(T_{in})_n$ along with the measured T_c profile.

As indicated earlier, we assumed that the heat transfer resistance across the interface between bulk fluid and pellet surface is negligible in arriving at the control policies of Eqs. (2-14) and (2-15). If there exists a significant temperature difference between bulk fluid and pellet surface, Eqs. (2-13) through (2-15) no longer hold. The discrepancy between h_c and h_n caused by the temperature difference can be compensated for by adjusting C_d as follows:

$$\tilde{C}_{d_i} = C_d + \alpha(\tilde{C}_{d_{i-1}} - C_{e_{i-1}}) \qquad i=1,2,... \tag{2-16}$$

$$C_{d_o} = C_d$$

where $\tilde{C}_{d_i}$ is the adjusted C_d when a step change in the inlet temperature, which is triggered by the bandwidth constraint, is made at the ith step and α is a proportionality constant with a value between zero and unity. Thus, for a given decrease in the outlet concentration from the desired value, the piecewise feedback control algorithm can be stated as follows:

$$-\int_{C_{in}}^{\tilde{C}_{d_i}} \frac{dC}{\tau k_a [T;(T_{in})_i] f(C,K_j)} = (H_c)_{i-1}$$

$$i=1,2,... \tag{2-17}$$

where $(H_c)_{i-1}$ is calculated from

$$(H_c)_{i-1} = -\int_{C_{in}}^{C_{e_{i-1}}} \frac{dC}{k_a [T;(T_{in})_{i-1}] f(C,K_j)} \quad i=1,2,... \tag{2-18}$$

$$(H_c)_o = 1$$

with the measured outlet concentration and inlet temperature. Here, $\tilde{C}_{d_i}$ is given by Eq. (2-16). Each time the outlet concentration reaches the allowed bandwidth, the new inlet

temperature $(T_{in})_i$ is calculated for the manipulation of the inlet temperature. All that is required for the feedback control is the global rate for catalyst at a reference state.

§2-2 Nature of Reactor Activity Factor

Before we proceed to multiple reactions, let us examine the nature of the reactor activity factor. By definition, it is an integrated value of local activity factor (Eq. 2-7). The local activity factor, which is the activity factor at a point in the reactor, can be obtained by solving pellet conservation equations. Instead of solving the conservation equations, we utilize the global rate obtained by Lee and Butt (1982) for a reaction affected by uniform deactivation and diffusion to get a clear picture of the local activity factor. The global rate for this case is

$$(R_G)_D = \frac{(1-\gamma)^{\frac{1}{2}}}{\frac{L}{[2D_e kI(C)]^{\frac{1}{2}}} - q} \tag{2-19}$$

where

$$I = \int_0^C g(\alpha)d\alpha \tag{2-20}$$

$$q = \frac{1.2E_a(-\Delta H)[2D_e kI]^{\frac{1}{2}}}{2h_m R_g T^2} \tag{2-21}$$

Here, γ is the fraction of catalyst deactivated, $g(C)$ the concentration dependence of the intrinsic rate of reaction, k the intrinsic rate constant, D_e the effective diffusivity, L the characteristic pellet length, and h_m the film heat transfer coefficient. The local activity factor can be obtained from the definition of Eq. (2-5):

$$h = \frac{(R_G)_D}{(R_G)_r} = \frac{(R_G)_D}{(R_G)_D\big|_{\gamma=1}} = (1-\gamma)^{\frac{1}{2}} \left[\frac{1-q}{1-(1-\gamma)^{\frac{1}{2}}q}\right] \qquad (2\text{-}22)$$

The same results hold (Lee and Ruckenstein, 1983) for non-uniform deactivation if γ is replaced with $\bar{\gamma}$, which is γ at the pellet surface, as long as $\bar{\gamma}$ is less than, say, 0.5.

It is clear from Eq. (2-22) that the local activity factor depends on γ and the quantity q which represents the heat transfer resistance across the bulk fluid-pellet surface interface. Since γ changes very little while the inlet temperature is raised to a new value, the magnitude of q determines whether h_c can be set to h_n. Therefore, the proportionality constant α in Eq. (2-16) can be chosen in accordance with the magnitude of q: for q much smaller than unity, the value of α can be set to zero, its value increasing with increasing q. Although the conclusion is made from the result for independent deactivation, the same should be valid for dependent deactivation since the factor causing the discrepancy between h_c and h_n is still the same, i.e. the heat transfer resistance across the interface, which q represents.

§2-3 Multiple Reactions

For simple parallel reactions, we can write

$$A \xrightarrow{1} b_1 B$$

$$A \xrightarrow{2} b_2 C$$

where b_1 and b_2 are the ratios of stoichiometric coefficients. We restrict our attention here to an adiabatic reactor for brevity since a nonadiabatic reactor can be treated in the same manner as shown for a single reaction. Let β denote the ratio of local activity factors, i.e., $\beta = h_2(z;t)/h_1(z;t)$, the reactor conservation equations can be written as:

$$\frac{dC_A}{dz} = -\tau h_1(z;t)\{k_{a_1} f_1(C_A, C_B) + \beta\, k_{a_2} f_2(C_A, C_B)\};$$

$$C_A\Big|_{z=0} = C_{A_{in}} \qquad (2\text{-}23)$$

$$\frac{dC_B}{dz} = b_1 \tau h_1(z;t) k_{a_1} f_1(C_A, C_B) \quad ; \quad C_B\Big|_{z=0} = C_{B_{in}} \qquad (2\text{-}24)$$

$$T = T_{in} + a_1(C_{A_{in}} - C_A) + a_2(C_B - C_{B_{in}}) \qquad (2\text{-}25)$$

where $a_1 = -\Delta H_2/\rho C_p$ and $a_2 = -\Delta H_1(1-\Delta H_2/\Delta H_1)\rho C_p b_1$. Equation (2-25) results when the heat balance equations are combined with the mass balance equations. Here the global rates for

the first and second reactions are expressed as $hk_{a_1} f_1(C_A, C_B)$ and $\beta hk_{a_2} f_2(C_A, C_B)$, respectively. If the same active sites are responsible for both reactions, the local activities are the same, and β is unity. Otherwise, we assume that β is a function of time but constant along the reactor, i.e., $\beta = \beta(t)$.

The reactor activity factor can be obtained in the same manner as for a single reaction:

$$H_1 = \int_0^1 h_1 dz = \int_{C_{B_{in}}}^{C_{B_e}} \frac{dC_B}{b_1 \tau k_{a_1} f_1(C_A, C_B)} \qquad (2\text{-}26)$$

where C_{B_e} is the outlet concentration of species B. As Eq. (2-25) indicates, the temperature can be expressed in terms of C_A and C_B for the calculation of H but C_A has to be related to C_B to carry out the integration. Combining Eqs. (2-23) and (2-24), we have

$$\frac{dC_A}{dC_B} = -\frac{1}{b_1}\left[1+\beta \frac{k_{a_2} f_2(C_A, C_B)}{k_{a_1} f_1(C_A, C_B)}\right]; \quad C_A\Big|_{C_B = C_{B_{in}}} = C_{A_{in}} \qquad (2\text{-}27)$$

which can be solved to obtain C_A as a function of C_B, $C_A = f(C_B)$, by Fourth Order Runge Kutta Method or Predictor-Corrector Method (Hornbeck, 1975). If β is unity, the solution is straightforward. Otherwise, the concentrations

measured at the outlet, C_{A_e} and C_{B_e}, can be used as an additional boundary condition, i.e., $C_A\Big|_{C_B = C_{B_e}} = C_{A_e}$, for Eq. (2-27) to obtain the value of β.

If species B is the desired species such that $(C_B)_d$ is the desired outlet concentration, the control policy similar to Eq. (2-14) can be written as

$$H_{1C} = \int_{C_{B_{in}}}^{(C_B)_d} \frac{dC_B}{b_1 \tau k_{a_{1o}} \exp\left[\frac{-E_a/R_g}{(T_{in})_n + a_1(C_{A_{in}} - C_A) + a_2(C_B - C_{B_{in}})}\right]} \cdot$$

$$f_1(C_A, C_B) \qquad (2\text{-}28)$$

which follows from Eq. (2-24). Here again, H_{1C} is the reactor activity factor for the reaction path 1 calculated just prior to a change in the inlet temperature. Equation (2-28) can be solved for $(T_{in})_n$ with the aid of Eq. (2-27). It is noted that $(T_{in})_n$ should also be used in Eq. (2-27) in the calculation.

Consider now consecutive reactions, for which we have

$$A \xrightarrow{1} b_1\, B \xrightarrow{2} b_2 C$$

With the same assumptions made for the parallel reactions, the conservation equations for an adiabatic reactor are

$$\frac{dC_A}{dz} = -\tau h(z;t) k_{a_1} f_1(C_A, C_B); \quad C_A\Big|_{z=o} = C_{A_{in}}$$

(2-29)

$$\frac{dC_B}{dz} = -\tau h(z;t)\ \{\beta k_{a_2} f_2(C_A,C_B) - b_1 k_{a_1} f_1(C_A,C_B)\} \quad ;$$

$$C_B\Big|_{z=0} = C_{B_{in}} \tag{2-30}$$

$$T = T_{in} + a_3(C_{A_{in}} - C_A) - a_4(C_B - C_{B_{in}}) \tag{2-31}$$

where $a_3 = (-\Delta H_1 - b\Delta H_2)/\rho C_p$ and $a_4 = -\Delta H_2/\rho C_p$. If we follow the same procedures as for the parallel reactions, we have for the reactor activity factor:

$$H_1 = \int_0^1 h_1 dz = -\int_{C_{A_{in}}}^{C_{A_e}} \frac{dC_A}{\tau k_{a_1}(T) f_1(C_A,C_B)} \tag{2-32}$$

The relationship between C_A and C_B resulting from Eqs. (2-29) and (2-30) is

$$\frac{dC_B}{dC_A} = -b_1 + \beta \frac{k_{a_2} f_2(C_A,C_B)}{k_{a_1} f_1(C_A,C_B)} \quad ; \quad C_B\Big|_{C_A = C_{A_{in}}} = C_{B_{in}} \tag{2-33}$$

The same procedures as for the parallel reactions can be used to calculate H from Eq. (2-32) with the aid of Eqs. (2-31) and (2-33).

The control policy for maintaining the desired outlet concentration of species B follows directly from Eq. (2-30) and the definition of H:

$$H_{1C}=-\int_{C_{B_{in}}}^{(C_B)_d}\frac{dC_B}{\tau\{\beta k_{a_2}[(T_{in})_n]f_2(C_A,C_B)-b_1k_{a_1}[(T_{in})_n]f_1(C_A,C_B)\}} \tag{2-34}$$

This can be solved for $(T_{in})_n$ with the aid of Eqs. (2-31) and (2-33). If, however, the control objective is to have maximum C_B at the outlet, the choice of $(C_B)_d$ in Eq. (2-34) must satisfy the necessary condition:

$$\left.\frac{dC_B}{dz}\right|_{z=1} = 0 \tag{2-35}$$

Substituting Eq. (2-35) into Eq. (2-30) gives

$$k_{a_2}(T_e)f_2[C_{A_e},(C_B)_d] = \beta b_1 k_{a_1}(T_e)f_1[C_{A_e},(C_B)_d] \tag{2-36}$$

which can be used to obtain $(C_B)_d$ with the aid of Eqs. (2-31) and (2-33). The new inlet temperature, $(T_{in})_n$ can then be obtained from Eq. (2-34).

The control policies of Eqs. (2-28) and (2-34) can be modified using Eq. (2-16) to obtain the piecewise algorithms similar to Eqs. (2-17) and (2-18).

CHAPTER 3

SIMULATION AND EXPERIMENTAL VERIFICATION

The theory in Chapter 2 is demonstrated here with a simulation of a model reaction system. The theory is also put to the test with a laboratory shell-and-tube reactor in which ethylene oxidation reactions take place over a silver catalyst. The catalyst undergoes sintering under the reaction conditions.

§3-1 Simulation of a Model Reaction System

For an illustration of the calculation of H and its use for the reactor control, we consider the reaction system studied by Lee and Butt (1982a), which is summarized in Tables 3-1 and 3-2. For the reaction taking place in an adiabatic reactor, which is affected by diffusion and uniform, independent poisoning, the intrinsic rate of deactivation r_p is given (Lee and Butt, 1982b) by

$$r_p = k_{p_a}(1-\gamma)N$$

where k_{p_a} is the rate constant evaluated at the pellet surface temperature and N is the concentration of poisoning species. With the use of reactor point effectiveness (Lee and Butt, 1982a), the reactor behavior can be simulated in a straightforward manner. The simulation results are used here as the process output for the purpose of illustrating

Table 3-1 Equations for the Model Reaction System

$$\frac{dC}{dz} = -\tau R_G \quad ; \quad C\Big|_{z=0} = C_{in}$$

$$\frac{dN}{dz} = -\tau k_{pa} N(1-\gamma) \quad ; \quad N\Big|_{z=0} = N_{in}$$

$$\frac{d\gamma}{dt} = -\frac{1}{Q} r_p = -\frac{1}{Q} k_{pa} N(1-\gamma); \quad \gamma\Big|_{t=0} = 0$$

where $$R_G = \frac{1/L}{\frac{1}{\left[2D_e k(1-\gamma)\int_0^C g(C)dC\right]^{1/2}} - \frac{1.2\,E_a(-\Delta H)}{2h_m R_g T^2}}$$

$$g(c) = \frac{C}{1+\xi C}$$

$$T = T_{in} - \left(\frac{-\Delta H}{pC_p}\right)(C - C_{in})$$

$$k = k_o \exp(-E_a/R_g T)$$

$$T_s = T + (-\Delta H)\, R_G L/h_m$$

$$k_{pa} = k_{po} \exp\,(-E_p/R_g T_s)$$

Table 3-2 Parameters For The Model Reaction System

$$k = \exp\left(-\frac{12{,}000}{T} + 14.6\right) \quad (1/s);\ E_a = 23.76 \text{ kcal/mol}$$

$$\xi = \exp\left(\frac{3{,}600}{T} + 3.86\right) \quad (cm^3/mol)$$

$$C_{in} = 1.81 \times 10^{-5} \text{ mol/cm}^3$$

$$\left(\frac{-\Delta H}{\rho C_p}\right) = 4 \times 10^7 \text{ K cm}^3/\text{mol};\quad -\Delta H = 5.04 \text{ kcal/mol}$$

$$h_m = 3.245 \times 10^{-4} \text{ cal/s.cm}^2\text{.K}$$

$$N_{in} = 5 \times 10^{-8} \text{ mol/cm}^3$$

$$Q = 10^{-4} \text{ mol/cm}^3 \text{ cat. pellet}$$

$$k_p = \exp\left(-\frac{7{,}000}{T} + 3.27\right);\ E_p = 13.86 \text{ kcal/mol}$$

$$D_p = 10^{-3} \text{ cm}^2/\text{s}$$

$$T_{max} = 1280\text{K}$$

$$X = 70\% \qquad \Delta X = 10\%$$

$$\tau = 20\text{s}$$

$$T_{in,o} = 691.8 \text{ K}$$

the feedback control given by Eqs. (2-16) through (2-18). The control problem is how the inlet temperature should be manipulated whenever the outlet conversion decreases to a certain level from the desired conversion (bandwidth). Note that the intrinsic rate of deactivation r_p is used here only to generate the process response. In the feedback control, r_p is treated as an unknown and only the on-line measurements (simulated temperature and concentration) are used to manipulate the inlet temperature. The constraints are the maximum reactor temperature allowed and the final time at which the catalyst is regenerated as the time when the final bandwidth becomes one-tenth of the initial bandwidth. These constraints are also given in Table 3-2 along with the desired outlet concentration (conversion) and the reactor size. The initial inlet temperature for fresh catalyst is the one corresponding to the specified reactor size (τ) and outlet conversion, which is 691.8K. Since the film heat transfer coefficient is quite small for the example problem and thus the value of q is relatively large, the proportionality factor β in Eq. (2-16) was set at 0.95.

The behavior of the model reactor resulting from the feedback control is shown in Figure 3-1. Initially, the inlet temperature is at its initial value and the outlet temperature, which is the maximum reactor temperature in

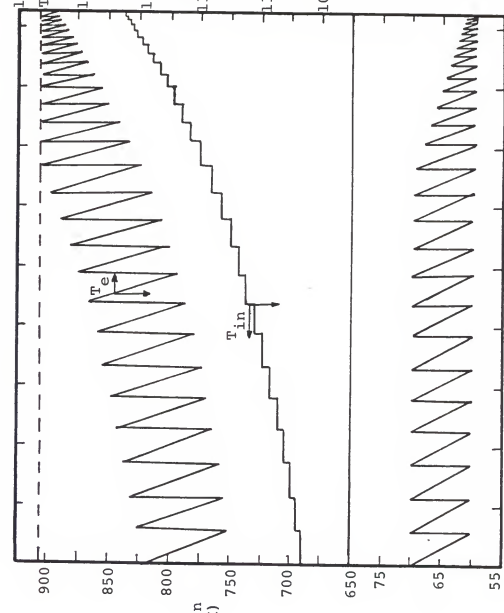

Figure 3-1. Temperature and Conversion Behavior of a Fixed-bed Subject to Inlet Temperature Manipulation

this case, is well below the maximum temperature allowed. Due to the deactivation, however, both the conversion and the outlet temperature decrease with time and the conversion eventually reaches the lower bound given by the bandwidth, triggering an adjustment of the inlet temperature. The new inlet temperature $(T_{in})_1$ calculated by the algorithm of Eqs. (2-16) through (2-18) is seen to bring the conversion back to the desired level, the actual value being 69.96% as opposed to the desired value of 70%. A bisection method was used for the calculation of $(T_{in})_j$. When the outlet temperature reaches the allowed maximum, which occurs at around $t = 2 \times 10^4$s, the conversion can no longer be brought back to the desired level due to the temperature constraint. Consequently the bandwidth decreases as time increases and eventually the bandwidth becomes less than one-tenth of the original bandwidth, resulting in the reactor shut-down for catalyst regeneration according to the constraint imposed. In practice, however, the conversion may be allowed to decrease below 60% when the maximum temperature is reached. In the example, the average conversion is essentially maintained at the middle of the bandwidth, which is 65%.

§3-2 Experimental Verification

We have shown the feasibility of control policies for the model reaction system. The theory has also been put to test using a shell-and-tube reactor. Experimental results obtained and comparisons with the theory are presented in this section.

§3-2-1 Catalyst Preparation

The catalyst used in this study of ethylene oxidation was silver supported on fused alumina. The quarter-inch-diameter alumina obtained from Norton Chemical Company (Catalog No. SA-5202) was crushed into 8-9 mesh (0.20~0.24cm) with a rod miller, washed with distilled water, and then dried in the furnace at 373 K overnight. These particles were porous with 0.7~1.3 m^2/g BET surface area and 1.9 g/cm^3 bulk density. The alumina was impregnated with an aqueous solution of lactic acid and silver oxide at 368 K for 90 minutes. The solution contained silver oxide, 85% lactic acid and distilled water in the ratio of 1:2:2 by weight. After impregnation the excess liquid was removed and the particles were heated in a furnace for 16 hours at 643 K to decompose the silver lactate to metallic silver. The catalyst was further stabilized by oxygenating at 573 K for 100 hours. Since the color of these pellets was not uniform, only those with lighter color were picked for the experiment. The weight gain indicated that the catalyst contained 12.4% silver. The oxygen chemisorption at 423 K was 36 μℓ/g.

§3-2-2 Experimental Apparatus

The reactor used for ethylene oxidation reactions was shell-and-tube type as shown in Fig. 3-2. The shell-and-tube section was 60.1 cm long with outside diameter (o.d.) of 3.81 cm for the shell and 1.19 cm for the tube.

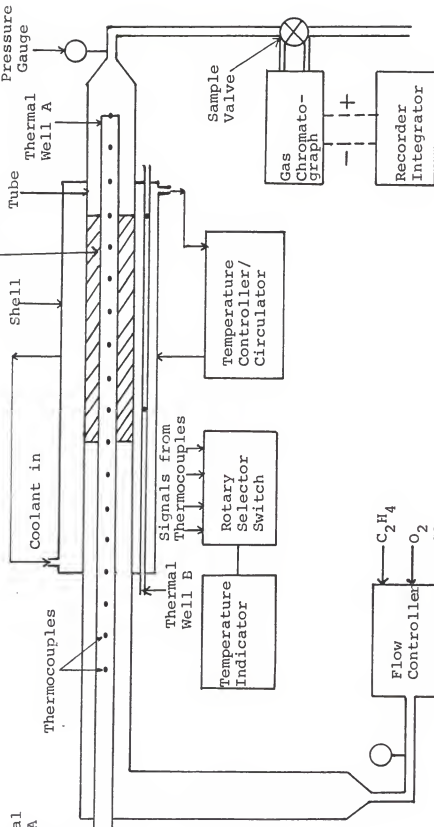

Figure 3-2. Experimental Apparatus for Ethylene Oxidation Reaction

One thermal well (A, 0.794 cm o.d.) ran axially into the tube, another (B, 0.0318 cm o.d.) into the shell. Silver catalyst was packed into the annular section between the tube and thermal well A. The shell-and-tube consisted of three segments (from left to right in Fig. 3-2): preheating zone (20.3 cm), reaction zone (35.6 cm) and outlet zone (5.1 cm). Glycerin was used as coolant which circulated through the shell side using a Haake HT22 temperature controller/circulator. A total of twenty temperatures were measured as shown in Fig. 3-2: eighteen in thermal well A and two in B.

All temperature points (thermocouples) were connected to a rotary selector switch which was in turn connected to a temperature indicator. The feed gases were introduced into the reactor at the desired mass flow rates and composition controlled by a multiple channel electronic mass flow controller. Two pressure gauges were installed, one at the inlet, the other at the outlet. The outlet composition was analyzed by a Tracor 550 gas chromatograph. The coolant flow rate was set high enough to maintain an essentially isothermal reaction zone. The reactor pressure was held constant at 1 atm.

§3-2-3 Determination of Kinetics

Ethylene oxidation involves a triangle reaction network (Spath and Handel, 1974; Dettwiler et al., 1979)

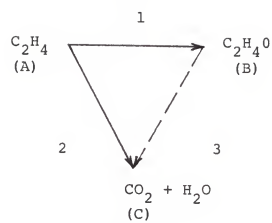

The oxidation of ethylene oxide (reaction path 3) is significant only at temperatures above 473 K (Dettwiler et al., 1979; Akella, 1983). Since the experiments were conducted in the temperature range between 448 and 468 K, only epoxidation and combustion of ethylene (reaction paths 1 and 2) need to be considered. A material balance in an isothermal fixed-bed can be written as

$$\frac{dF_A}{dz} = -h_1(r_1 + \beta r_2)W \quad ; \quad F_A\Big|_{z=0} = F_{Ao} \qquad (3\text{-}1)$$

$$\frac{dF_B}{dz} = h_1 r_1 W \quad ; \quad F_B\Big|_{z=0} = F_{Bo} = 0 \qquad (3\text{-}2)$$

where F_A and F_B are the molar flow rates for ethylene and ethylene oxide, respectively, and W is the weight of the catalyst. Here r_1 and r_2 are the intrinsic rates for the reaction paths 1 and 2. The mechanism of ethylene oxidation is still controversial. Under the condition of constant oxygen partial pressure, however, the following Langmuiur-Hinshelwood rate expressions are reported by most investigators (Dettwiler et al., 1979):

$$r_1 = \frac{k_1 k_q p_A}{1+k_q p_A} \tag{3-3}$$

$$r_2 = \frac{k_2 k_q p_A}{1+k_q p_A} \quad \text{(mol/s·g-cat.)} \tag{3-4}$$

where p_A is the partial pressure of ethylene and k_q is an adsorption equilibrium constant. Since the catalyst particles are small, there is no diffusion limitation and the intrinsic rates are essentially the same as the global rates.

Let x and y be the conversion and yield in the reactor, i.e. $x = (F_{Ao} - F_A)/F_{Ao}$ and $y = (F_B - F_{Bo})/F_{Ao}$. Then, Eq. (3-1) can be rendered dimensionless with the aid of Eqs. (3-3) and (3-4):

$$\frac{dx}{dz} = \frac{W}{F_o y'_{Ao}} \frac{h_1(k_1+\beta k_2)\ k_q p y'_{Ao}(1-x)}{1+k_q p y'_{Ao}(1-x)} \ ; \ x\Big|_{z=0} = 0 \tag{3-5}$$

where F_o is the molar flow rate of reactant mixture and y'_{Ao} is the mole fraction of ethylene, both at the inlet of the reactor. The ideal gas law has been applied to obtain Eq. (3-5). The reactor activity factor for the reaction path 1, H_1 can be obtained by rearranging Eq. (3-5) and integrating from the reactor inlet to the outlet:

$$H_1 = \int_0^1 h_1 dz = \frac{k_q p y'_{Ao} X - \ell n(1-X)}{(k_1+\beta k_2) k_q p W/F_o} \tag{3-6}$$

where X is the conversion at the outlet.

Dividing Eq. (3-1) by (3-2) and nondimensionalization gives

$$\frac{dx}{dy} = 1 + \beta\frac{r_2}{r_1} = 1 + \beta\frac{k_2}{k_1} \; ; \quad x\Big|_{y=o} = 0 \tag{3-7}$$

Since the right hand side of Eq. (3-7) is constant throughout the isothermal reactor, Eq. (3-7) can be integrated from the reactor inlet to the outlet to give

$$\frac{X}{Y} = 1 + \beta\frac{k_2}{k_1} \tag{3-8}$$

where Y is the yield at the outlet.

Equations (3-6) and (3-8), which are the integrated versionsof Eqs. (2-26) and (2-27), can be used for both the feedback control described in Section §2-3-3 and the determination of kinetics. Before proceeding to the control policies, consider the kinetics first. It is convenient to choose the activity of the catalyst at the time kinetic data are taken as the reference state activity. Then, both h_1 and β are unity by definition, and Eqs. (3-6) and (3-8) can be rearranged as

$$\left[\ell n\ \frac{1}{1-X}\right] = -k_q{}^p\left[y'_{Ao}X\right] + \frac{k_1 k_q{}^p W}{F_o}\left(\frac{X}{Y}\right) \tag{3-9}$$

and $$k_2 = k_1\left(\frac{X}{Y} - 1\right) \tag{3-10}$$

It has been shown (Akella, 1983) that the selectivity, defined as S = Y/X, is fairly independent of ethylene

partial pressure but is dependent on the reaction temperature. This can also be seen from Eq. (3-8) where the left hand side is 1/S and the right hand side depends only on temperature. Thus, at any given temperature, X/Y is constant, and Eqs. (3-9) can be used to obtain k_q and $k_1 k_q$ by a linear regression of $(\ell n \frac{1}{1-X})$ on $(y'_{Ao} X)$. The rate constant k_2 can then be calculated from Eq. (3-10). By definition and the stoichiometric relationships, the conversion and yield at the reactor outlet can be related to the inlet and outlet gas compositions as

$$X = 1 - \frac{y'_{Al}}{y'_{Ao}} \tag{3-11}$$

$$Y = X - \frac{y'_{Cl}}{2y'_{Ao}} \tag{3-12}$$

where y'_{Ao} and y'_{Al} are the mole fractions of ethylene at the inlet and outlet, respectively, y'_{Cl} is the mole fraction of carbon dioxide at the outlet.

We have shown that at a given temperature, the rate constants, k_1 and k_2, and the absorption equilibrium constant, k_q, can be determined from the inlet and outlet gas compositions, y'_{Ao}, y'_{Al} and y'_{Cl}, using Eqs. (3-9) through (3-12). The kinetic data for ethylene oxidation reactions are given in Table 3-3. The reactor was maintained isothermal by controlling the coolant flow rate at a high level. Due to the low ethylene concentration and the high coolant flow rate, the heat generated by the reactions was removed immediately by the coolant. The oxygen composition in the feed gas was maintain at 20% for all runs, with

Table 3-3 Kinetic Data for Ethylene Oxidation Reactions

RUN	T(K)	y'_{Ao}(%)	y'_{Al}(%)	y'_{Cl}(%)	X(%)	Y(%)	S(%)	$\bar{S}$(%)
1	448	4.00	3.36	.487	16.04	9.95	62.0	62.4
2	448	6.00	5.28	.537	11.93	7.45	62.5	
3	448	8.00	7.26	.551	9.23	5.79	62.7	
4	458	4.00	3.10	.718	22.51	13.53	60.1	59.8
5	458	6.00	5.01	.788	16.55	9.98	60.3	
6	458	8.00	6.94	.869	13.26	7.83	59.0	
7	468	4.00	2.77	.971	30.79	18.65	60.6	59.7
8	468	6.00	4.60	1.12	23.31	14.00	60.1	
9	468	8.00	6.52	1.23	18.48	10.81	58.5	

F_o = 100 ml/min

P = 1 atm

W = 78.34 g

helium as the diluent. Given in Table 3-4 are the results of the linear regression of $(\ell n \frac{1}{1-X})$ on $(y'_{Ao}X)$ for each temperature. The values of $(\ell n \frac{1}{1-X})$ calculated from the regression model, $(\ell n \frac{1}{1-X})_{cal}$, are included in the table for comparison. The percent error in the table was calculated from

$$\text{Error} = \left(\frac{\ell n \frac{1}{1-X}}{(\ell n \frac{1}{1-X})_{Cal}} - 1 \right) \times 100\% \qquad (3\text{-}13)$$

The constants k_1 and k_q were calculated from the slope and intercept of the regression line, while k_2 was calculated from Eq. (3-10). The values of these rate constants are given in Table 3-4 along with the coefficients of correlation. Note that the average selectivity, $\bar{S}$, given in the last column of Table 3-3 was used to calculate k_1 and k_q.

It was assumed that the temperature dependence of the rate and equilibrium constants are all of the Arrhennius form:

$$k_i = A_i \exp(- E_i/R_gT) \quad i=1, 2, q \qquad (3\text{-}14)$$

The activation energies and pre-exponential factors were obtained from linear regressions of $\ell n\ k_i$ on $1/T$. The results are given in Table 3-5.

The experimental results show that the kinetics of ethylene oxidations reactions can be well represented in the form of Eqs. (3-3) and (3-4) with the following rate constants and equilibrium constant:

Table 3-4 Results of Linear Regression of $\ell n \frac{1}{1-X}$ on $y'_{Ao}X$

RUN	T (K)	$y'_{Ao}X$ ($\times 10^{-3}$)	$\ell n \frac{1}{1-X}$ ($\times 10^{-1}$)	$\left(\ell n \frac{1}{1-X}\right)_{cal}$ ($\times 10^{-1}$)	Error (%)	k_1 ($\times 10^{-9}$)	k_2 ($\times 10^{-9}$)	k_q ($\times 10$)	Corr. Coeff.
1	448	6.417	1.749	1.766	-1.0	4.797	2.890	7.675	-0.9863
2	448	7.156	1.270	1.198	6.0				
3	448	7.384	0.968	1.023	-5.3				
4	458	9.005	2.551	2.526	1.0	6.631	4.453	7.089	-0.9960
5	458	9.932	1.810	1.869	-3.2				
6	458	10.61	1.423	1.388	2.5				
7	468	12.32	3.680	3.697	-0.4	9.457	6.378	6.556	-0.9985
8	468	13.99	2.654	2.603	2.0				
9	468	14.79	2.043	2.078	-1.7				

Table 3-5 Results of Linear Regression of $\ell n\ k_i$ on 1/T

i	T	1/T ($\times 10^{-3}$)	$\ell n\ k_i$ (x10)	$(\ell n\ k_i)^{\dagger}_{cal}$ (x10)	Error (%)	A_i	E_i/R_g	Corr. Coeff.
1	448	2.232	-1.196	-1.916	-0.0	3.618×10^{-2}	7.098×10^{3}	-0.9991
	458	2.183	-1.883	-1.882	0.1			
	468	2.137	-1.848	-1.849	-0.1			
2	448	2.232	-1.966	-1.967	-0.1	3.038×10^{-1}	8.279×10^{3}	-0.9980
	458	2.183	-1.923	-1.920	0.2			
	468	2.137	-1.887	-1.888	-0.1			
q	448	2.232	0.4340	0.4340	0.0	1.942	-1.647×10^{3}	-0.9998
	458	2.183	0.4261	0.4260	0.0			
	468	2.137	0.4183	0.4183	-0.0			

†calculated from regression model

$$k_1 = 3.618 \times 10^{-2} \exp(-7098/T) \quad \text{(mol/s.g-cat)}$$

$$k_2 = 3.038 \times 10^{-1} \exp(-8279/T) \quad \text{(mol/s.g-cat)}$$

$$k_q = 1.942 \exp(1641/T) \quad \text{(1/atm)} \qquad (3\text{-}15)$$

$$0.04 \text{ atm} \leq P_{Ao} \leq 0.08 \text{ atm}$$

$$448 \text{ K} \leq T \leq 468 \text{ K}$$

The comparisons made in Table 3-6 between the experimental conversions and those predicted by the kinetic model show very good agreements, the maximum error being 1.9%. The same can be concluded for the yield and selectivity. It is seen from the table that the maximum errors are 2.3 and 3.4% respectively for the yield and selectivity.

The experiments for the kinetic data lasted 9 hours. An additional run carried out right after the period with the same conditions as in Run No. 2 gave almost the same conversion and yield as shown in Fig. 3-3 at t = o and t = 9 hr. This is a good indication that no significant deactivation had occurred during the kinetic experiments.

§3-2-4 Experimental Verification of the Control Policy

The shell-and-tube reactor at the end of the kinetic experiments was allowed to run continuously to verify the feedback control policy presented in Chapter 2. The feed rate was controlled at 100 ml/min with the ethylene, oxygen and helium concentrations of 6, 20 and 74%, respectively,

Table 3-6 Comparison Between Experimental Data and Kinetic Model

RUN	X†	X_{cal}*	Error§	Y	Y_{cal}	Error	S	S_{cal}	Error
1	16.04	15.94	0.6	9.95	9.96	-0.0	62.0	62.4	-0.6
2	11.93	11.70	1.9	7.45	7.30	2.0	62.5	62.4	0.0
3	9.23	9.22	0.1	5.79	5.76	0.5	62.7	62.4	0.4
4	22.51	22.30	0.9	13.53	13.62	-0.6	60.1	61.1	-1.6
5	16.55	16.55	0.0	9.98	10.11	-1.2	60.3	61.1	-1.2
6	13.26	13.12	1.1	7.83	8.01	-2.3	59.0	61.1	-3.4
7	30.79	30.53	0.8	18.65	18.25	2.2	60.6	59.8	1.4
8	23.31	22.98	1.4	14.00	13.73	2.0	60.1	59.8	0.5
9	18.48	18.34	0.8	10.81	10.96	-1.4	58.5	59.8	-2.1

†Experimental data

*Kinetic model

§Error = $(X/X_{cal}-1)\cdot 100\%$

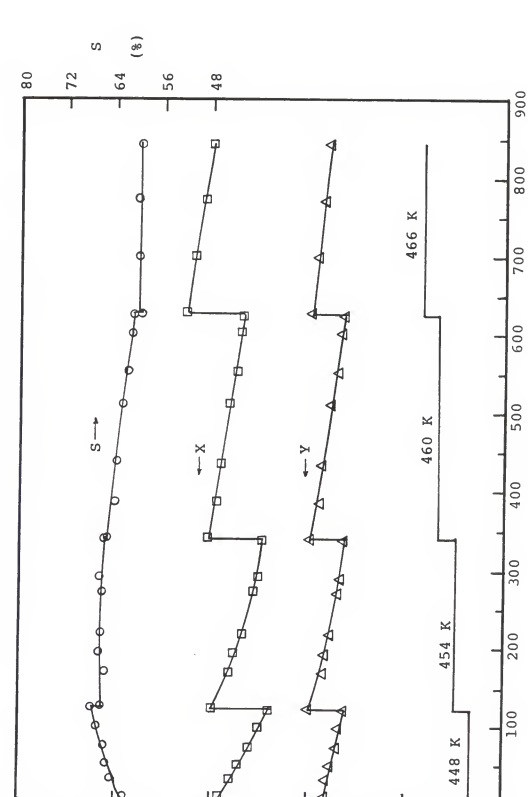

Figure 3-3. Conversion, Yield and Selectivity Behavior for Ethylene Oxidation Reaction

The temperature was kept constant at 448 K. The outlet gas compositions were analyzed daily and the corresponding conversion and yield were calculated. The control policy was that of maintaining the yield of ethylene oxide at 8% in a piecewise manner. The bandwidth was set in such a way that an adjustment was made whenever the yield decreased to 6.5%. The temperature adjustments and the corresponding reactor behavior over a period of 35 days are shown in Fig. 3-3. The first temperature adjustment occurred at t = 120 hr. at which time the yield dropped down to 6.5%. This triggered an adjustment of the temperature in accordance with the specification of the bandwidth.

Consider the temperature adjustment, in particular the procedures of calculating the new temperature which will bring the yield back to the desired level. The value of β required to calculate H_1 from Eq. (3-6) is obtained directly from the experimental values of the conversion and yield at the current temperature. This in turn is used in Eq. (3-6) to calculate the current reactor activity factor for the reaction path 1, H_{1c}. Rewriting Eq. (3-6) for the new temperature and using the relationship $H_{1c} = H_{1n}$ yields

$$H_{1c} = \left[\frac{k_q P y'_{Ao} X_d - \ell n(1 - X_d)}{(k_1 + \beta k_2) k_q PW/F_o} \right]_n \qquad (3\text{-}16)$$

Here, the subscript n denotes the new temperature and X_d is the desired conversion. Since local activities change little during the short period of temperature adjustment, β, by definition, also changes little. This means that the same β obtained from Eq. (3-8) can be used in Eq. (3-16) to calculate the new temperature. If the conversion X_d is the one to be controlled, then Eq. (3-18) can be used to calculate T_n, since it is the only unknown in Eq. (3-18). In this case, however, the yield Y_d is to be controlled. Hence, we need an additional relationship between X_d and Y_d. This relationship can be obtained by rewriting Eq. (3-8) for the new temperature

$$\frac{X_d}{Y_d} = 1 + \beta\left(\frac{k_2}{k_1}\right)_n \qquad (3\text{-}17)$$

This relationship was used for the calculation of the new temperature in the experiment.

The experiments were conducted over a period of 884 hours. As shown in Fig. 3-3, the first adjustment was made at t = 120 hr. The temperature was raised to 454 K, which brought the yield to 7.95% for the desired yield of 8%. Two additional temperature adjustments were made at t = 336 hr. and t = 624 hr. The experimental values of the yield of ethylene oxide resulting from the temperature adjustements were both 7.92%. The behavior of conversion and selectivity are also shown in Fig. 3-3. It is interesting to observe that

the selectivity increases at 448 K, remains almost constant at 454 K and then decreases at 460 and 466 K. This behavior can be explained in terms of H_1 and H_2. As shown in Fig. 3-4, H_1 and H_2 decrease with different speeds, resulting in the observed selectivity behavior. The results given in the figure show excellent agreements between the theory and the experiment.

The experimentally determined values of H_1 and H_2 were fitted to an nth order deactivation kinetics using a non-linear regression. The results are

$$\frac{dH_1}{dt} = - k_{D_1} H_1^{m_1} = -5.018 \times 10^5 \exp(-8879/T) H_1^{3.87}$$

$$\frac{dH_2}{dt} = - k_{D_2} H_2^{m_2} = - 1.936 \times 10^{-8} \exp(5707/T) H_2^{6.19}$$

The experimental values are plotted in Fig. 3-4 along with the calculated values, which are shown as solid curves.

§3-3 Concluding Remarks

We have shown in Section §3-1 the feasibility of the feedback control policies by simulating an adiabatic fixed-bed where a single reaction affected by diffusion and poisoning takes place. The feedback control policies have also been put to test with a laboratory isothermal fixed-bed where multiple reactions affected by sintering take place.

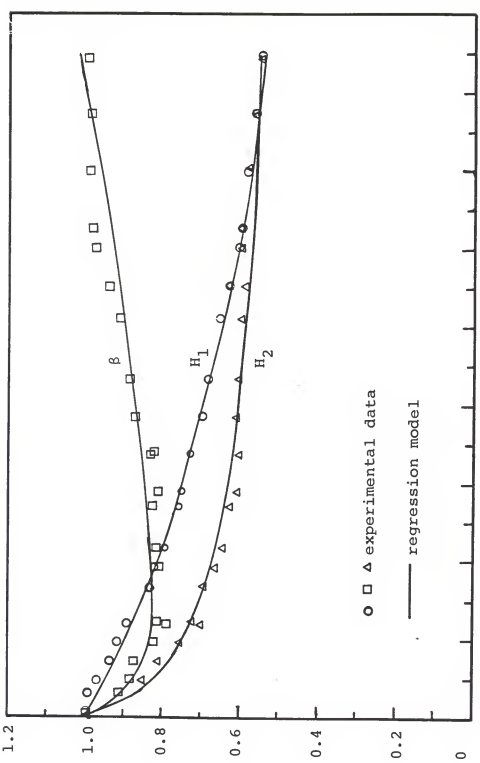

Figure 3-4. Activity Behavior for Ethylene Oxidation Reaction

The results in Fig. 3-1 and 3-3 show that one can indeed maintain the conversion or yield at the desired level with good accuracy. It is noted in this regard that the control policies can also be used to control the conversion or yield in any desired manner, since X_d or Y_d can be changed each time the temperature is raised.

The accuracy of the feedback control depends mostly on the on-line measurements (X and Y) but slightly on the reference-state kinetics determined. For example, at t = 624 hr., (as shown in Fig. 3-3 when T is adjusted from 460 to 466 K), 5% error in the determination of yield results in 1.7K difference in the new temperature calculated, while 5% error in activation energy for reaction path 1 (E_1) leads to only 0.3 K difference. In calculating new temperature by use of Eq. (3-16), the on-line measurements of conversion and yield are used only on the left hand side of the equation, while the activation energy E_1 is used on both sides. Thus, any error in E_1 is likely to be cancelled out from both sides of the equation. This is a good indication that the feedback control is applicable even when some uncertainty exists in the kinetic model.

CHAPTER 4

OPTIMAL PIECEWISE CONTROL

The control policies discussed in the previous chapters are all piecewise type, i.e. the control actions are taken at discrete intervals. The optimal control problems for reactors affected by catalyst deactivation have been the subject of several studies (Chou et al., 1967; Szepe and Levenspiel, 1968; Crowe, 1970), and a constant conversion policy has been proved to be optimal for a single irreversible reaction with concentration-independent deactivation. These studies deal only with the continuous control, which is essentially the piecewise control with an infinite number of steps. However, the feasibility of extending the optimal continuous control policies to piecewise control schemes with a finite number of steps remains questionable. In this chapter, a solution method for the optimal piecewise control is developed and a comparison between continuous and piecewise control is made.

§4-1 Problem Statement and Solution Method

Consider an isothermal fixed-bed where a single irreversible reaction affected by catalyst deactivation takes place. The temperature is to be adjusted in steps from T_1 to

T_n as shown in Fig. 4-1. The pseudo steady-state balance equations can be written as

$$\frac{dh}{dt} = g(T_1, T_2, \ldots T_n, h) \; ; \; h\Big|_{t=0} = 1 \qquad (4\text{-}1)$$

$$X = f(T_1, T_2, \ldots T_n, h) \qquad (4\text{-}2)$$

where h is the activity of the catalyst, X is the conversion at the outlet of the reactor, and g represents the dependence of deactivation rate on the temperatures (T) and activity (h). Equation (4-2) is obtained by integrating the mass balance equation from the inlet to the outlet of the reactor.

The optimization problem is to maximize the total amount of feed converted over a fixed total reaction time, t_n, by choosing the best set of temperatures, $[T_1, T_2, \ldots, T_n]$. That is

$$J^* = \max_{T_i} J \qquad i = 1, 2, \ldots n \qquad (4\text{-}3)$$

with

$$J = \frac{1}{t_n} \int_0^{t_n} X dt = \frac{1}{t_n} \sum_{i=1}^{n} \int_{t_{i-1}}^{t_i} X dt \qquad (4\text{-}4)$$

and subject to

$$T_{min} \leq T_i \leq T_{max}$$

$$\Delta t = t_i - t_{i-1} = \text{constant} = \frac{t_n}{n} \quad i = 1, 2, \ldots n \qquad (4\text{-}5)$$

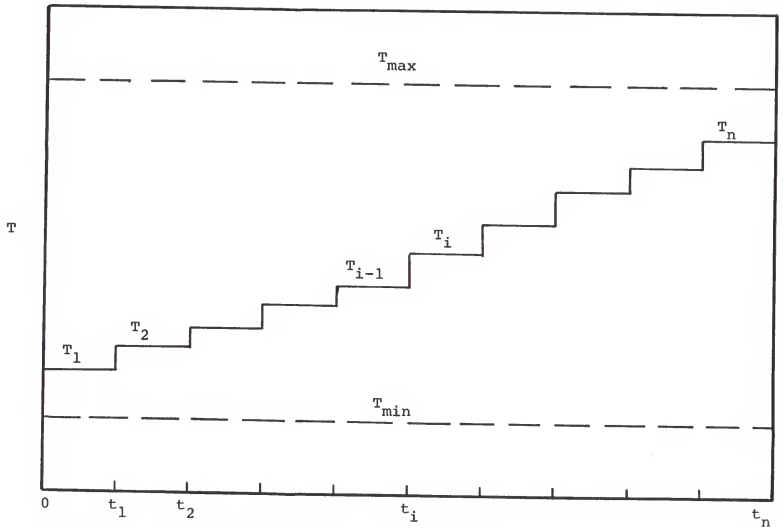

Figure 4-1. Temperature Behavior for a Piecewise Control

Equation (4-1) can be solved, analytically or numerically, to give

$$h = h(T_1, T_2, \ldots T_n, t) \tag{4-6}$$

Integrating Eq. (4-4) with the aid of Eqs. (4-2) and (4-6) yields

$$J = J(T_1, T_2, \ldots T_n) \tag{4-7}$$

Thus, the optimal piecewise temperature control problem of Eqs. (4-3) through (4-5) is a multivariable optimization problem searching for n variables (T_1, T_2, ... T_n), rather than a variational calculus problem searching for a continuous function (T(t)). The latter is often encountered in problems dealing with optimal continuous control. The stationary point of J can be obtained either by applying the necessary conditions

$$\frac{\partial J}{\partial T_i} = 0 \qquad i = 1, 2, \ldots n \tag{4-8}$$

and then solving these n nonlinear equations numerically, or by direct numerical search (Beveridge and Schechter, 1970). It is worth noting that even for the simplest first order reaction and deactivation, the expression for J is still very complex and the partial derivatives in Eq. (4-8) are difficult to obtain analytically. Therefore, direct numerical search is a better method for obtaining the optimal temperature policy, T_1^*. T_2^*..., T_n^*. The optimal temperature policy leads directly to the optimal conversion policy through Eq. (4-2) with the aid of Eq. (4-1).

§4-2 Optimal Piecewise Control Policies

As an illustration, the optimal piecewise control problem of Eqs. (4-1) through (4-5) was solved for a model reaction system of first order irreversible reaction with first order deactivation (Table 4-1). The multivariable optimization problem was solved by direct numerical search using the ZXMWD subroutine from International Mathematical and Statistical Libraries (IMSL). The ZXMWD subroutine is used for obtaining the global minimum or maximum for a multivariable function with constraints. The constrained maximization problem of

$$J^* = \max_{T_1,\ldots T_n} J(T_1, T_2,\ldots T_n) \tag{4-9}$$

with

$$T_{min} \leq T_i \leq T_{max} \quad i = 1, 2, \ldots n$$

is transformed in ZXMWD subroutine to an equivalent, but unconstrained problem

$$J^* = \max_{\bar{T}_1,\ldots \bar{T}_n} J[T_{min}+(T_{max}- T_{min})\sin^2\bar{T}_1,\ldots,T_{min} + (T_{max} - T_{min})\sin^2\bar{T}_n] \tag{4-10}$$

where $\bar{T}_i$ is the transformed function of T_i and is now unconstrained. With this transformation, each possible global maximum, including any on the boundary, is transformed into a local maximum (Box, 1966).

Shown in Figure 4-2 are the optimal piecewise control policy for the model reaction. The optimal temperature

Table 4-1 Equations and Parameters for a Model Reaction System for Optimal Piecewise Control

$$\frac{dh}{dt} = - k_D h \qquad ; \qquad h\Big|_{t=0} = 1$$

$$X = 1 - \exp(-\tau k_1 h)$$

$$k_D = A_D \exp\left(- \frac{G_D}{T}\right)$$

$$k_1 = A_1 \exp\left(- \frac{G_1}{T}\right)$$

$$T(t) = T_i \quad \text{for} \quad (i-1)\frac{t_n}{n} \leq t < i\frac{t_n}{n} \; ; \quad i = 1,2,\ldots n$$

$$T_{min} \leq T_i \leq T_{max} \qquad ; \quad i = 1,2,\ldots n$$

$A_D = 5.00 \times 10^6 \ hr^{-1}$ $\qquad$ $A_1 = 5.00 \times 10^6 \ S^{-1}$

$G_D = 1.25 \times 10^4 \ K$ $\qquad$ $G_1 = 1.00 \times 10^4 \ K$

$t_n = 2000 \ hr$ $\qquad$ $\tau = 20 \ S$

$T_{min} = 473 \ K$

$T_{max} = 573 \ K$ in Figs. (4-2), (4-3) and (4-5)

$= 673 \ K$ in Figs. (4-4), (4-6) and (4-7)

$n = 10$ in Figs. (4-2) through (4-6)

$=$ varies in Fig. (4-7)

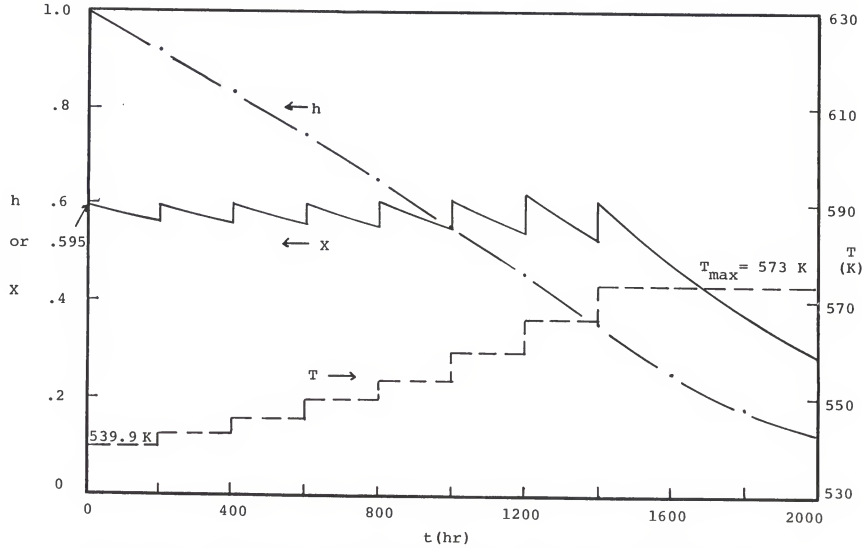

Figure 4-2. Optimal Piecewise Control Policies for the Model Reaction, T_{max} = 573 K

policy is to step the temperature up from 539.9 K until it reaches T_{max} (573 K) at t = 1400 hr. and then to keep it at that level as shown in the figure. The corresponding conversion zigzags with increasing bandwidth until the temperature reaches its upper limit. Due to catalyst deactivation the conversion decreases in each time interval while the temperature remains constant. It is of interest to note that each temperature increase gives a conversion peak which is slightly higher than the previous one, i.e.

$$X_n(t_i) > X_n(t_{i-1}) \text{ for } T < T_{max}$$

where n denotes the new conversion immediately following the temperature adjustment. In other words, the optimal piecewise policy is an increasing conversion policy, rather than a constant conversion policy which is the optimal for continuous control (Crowe, 1970). The optimal continuous control policy for the same model reaction is shown in Fig. 4-3 for comparison. It is obtained by one-dimensional search of the optimal initial temperature with the aid of the constant conversion policy. It can be seen from the figure that the optimal continuous policy is a constant conversion policy followed by a constant temperature policy at T_{max}. Comparison between Fig. 4-2 and 4-3 shows that the temperature in the continuous control starts 1.3 K lower than in the piecewise scheme and reaches the upper limit 42 hours later. It can also be seen that the conversion in the continuous control is lower than the original conversion in the piecewise control, but stays in the zigzag zone of the piecewise scheme. The corresponding activity behavior is also plotted in Figs. 4-2 and 4-3.

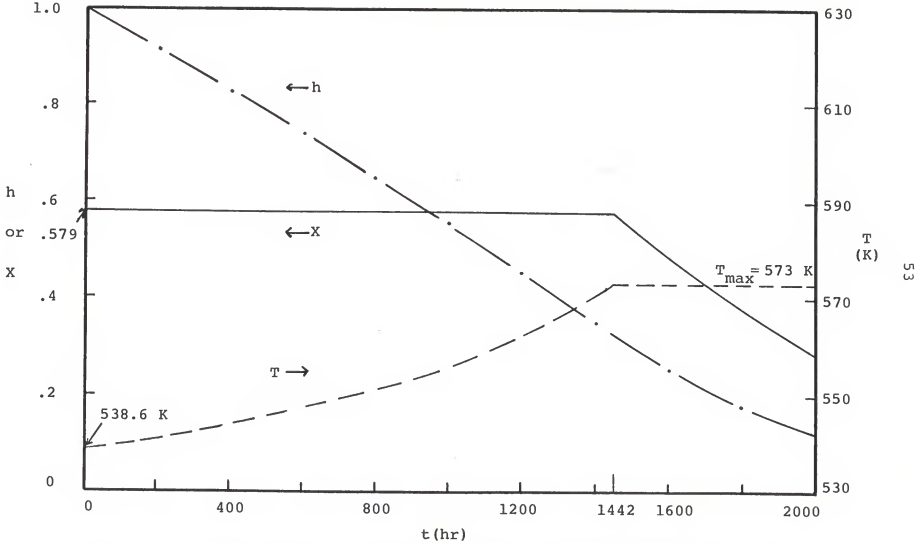

Figure 4-3. Optimal Continuous Control Policy for the Model Reaction, T_{max} = 573 K

Another major difference between the piecewise and the continuous control is that although the temperature in the optimal continuous control always ends at its upper limit for the model reaction studied here (Crowe, 1970), the temperature in the optimal piecewise control may end at a temperature below the upper limit. This is shown in Fig. 4-4 where the final temperature is 621.3 K, far below the upper limit, 673 K. However, the final temperature will approach 673 K as the number of control steps, n, increases.

A comparison of performance indices calculated from Eq. (4-4) for seven different control policies is given in Table 4-2 with T_{max} = 573 K and 673 K. The performance indices calculated with the optimal piecewise temperature control policy, T^*, are listed in Entry 1. In Entries 2 and 3, the temperature control policies are 1 K higher and lower, respectively, than T^*, but still within the interval $[T_{min}, T_{max}]$. The control policy T_c^* in Entry 4 is obtained by solving the same optimization problem with an additional constraint of constant conversion. Note that by applying the constant-conversion constraint, the multivariable optimization problem of Eq. (4-9) is simplified to a single variable optimization problem

$$J_c^* = \max_{T_1} J_c(T_1) \tag{4-11}$$

since T_2, T_3,... and T_n are fixed when T_1 is specified. Here subscript c denotes the performance index obtained under the constant-conversion constraint. The performance

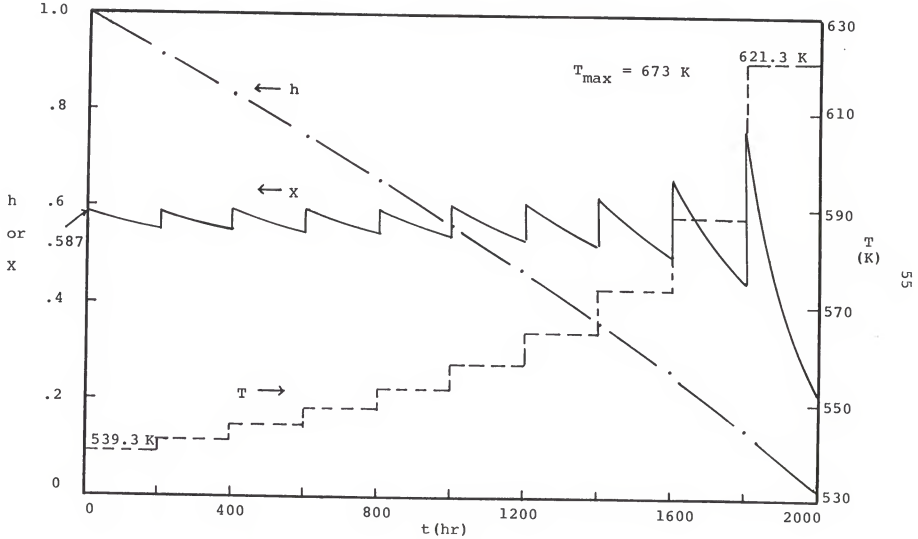

Figure 4-4. Optimal Piecewise Control Policy for the Model Reaction, T_{max} = 673 K

Table 4-2 Comparison of Performance Indices for Different Control Policies

Entry	Temperature Control Policy	T_{max} = 573 K		T_{max} = 673 K	
		J_i	$\tilde{J}_i^{\S}$	J_i	$\tilde{J}_i^{\S}$
1	$T = T^*$	0.53512	100.00	0.55855	100.00
2	$T = T^* + 1$	0.53498	99.97	0.55937	99.97
3	$T = T^* - 1$	0.53498	99.97	0.55837	99.97
4	$T = T_c^{*\dagger}$	0.53503	99.98	0.55628	99.59
5	$T = T_t^{*\dagger\dagger}$	0.49219	91.98	0.49219	88.12
6	$T = T_{max}$	0.44007	82.24	0.04823	8.63
7	$T = T_{min}$	0.06268	11.71	0.06268	11.22

$\S$ $\tilde{J}_i = J_i/J_1 \times 100\%$

$\dagger$ with constant-conversion constraint

$\dagger\dagger$ with constant-temperature constraint

indices obtained from Eq. (4-11) are listed in Entry 4. In Entries 5 through 7, the temperature policies are all constant with respect to time. It can be seen from the table that T^* (the optimal temperature policy shown in Fig. 4-2) is indeed the optimal temperature control policy, since all the other policies result in smaller values of the performance index.

The single-variable optimization problem of Eq. (4-11) was solved numerically using Fibonacci search (Beveridge and Schechter, 1970). The results are shown in Fig. 4-5 for T_{max} = 573K and in Fig. 4-6 for T_{max} = 673 K. It can be seen from the figures that the conversion is brought back to the initial conversion each time the temperature is adjusted.

§4-3 Concluding Remarks

A comparison between the optimal performance indices obtained with and without constant-conversion constraint is shown in Fig. 4-7 as a function of the number of control actions (n). It is seen that as n approaches infinity, J^* and J_c^* approach the same asymptotic value (0.56556 for the model reaction with T_{max} = 673 K). This indicates that the continuous control (which corresponds to an infinite number of piecewise control actions) is superior to the piecewise control in terms of the performance index. On the other hand, $J^* > 99.5\%$ when n>21 as shown in Fig. 4-7, implying that the piecewise control is almost as good as the continuous control if the number of control actions is large

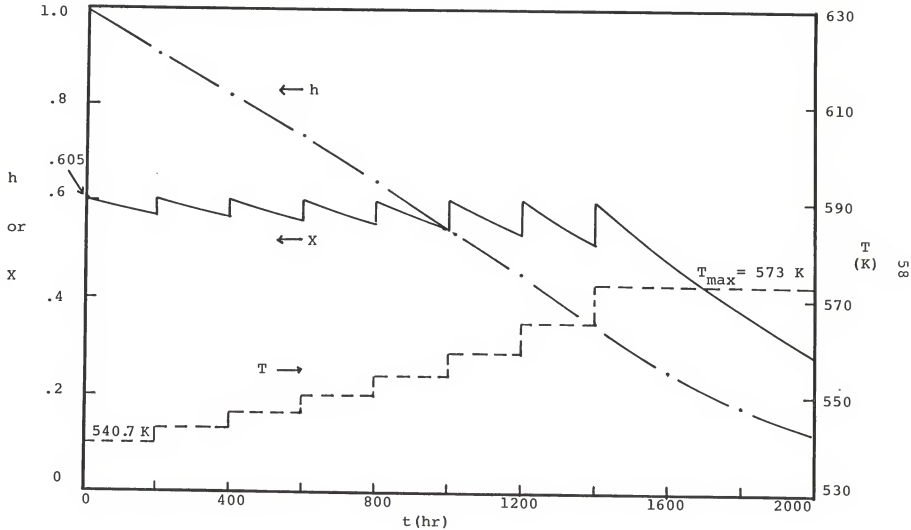

Figure 4-5. Optimal Piecewise Control Policy with Constant Conversion, T_{max} = 573 K

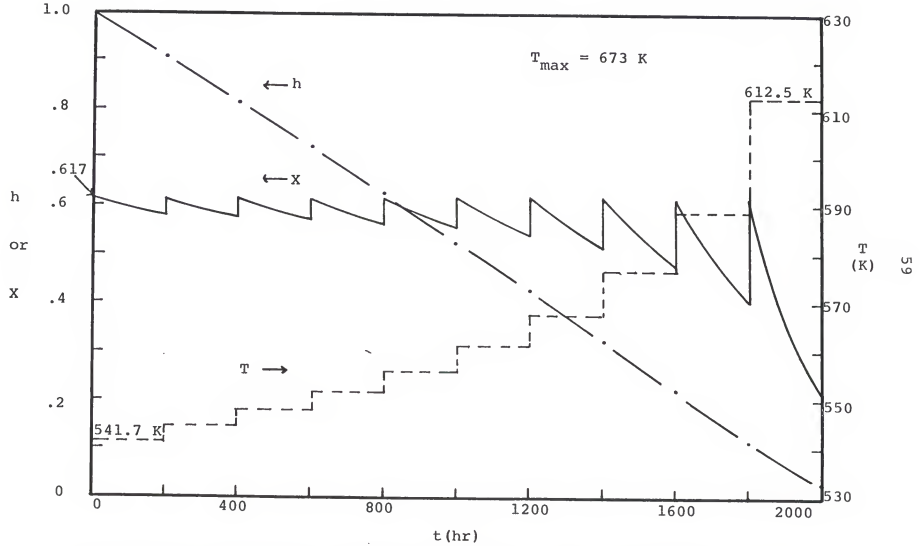

Figure 4-6. Optimal Piecewise Control Policy with Constant Conversion, T_{max} = 673 K

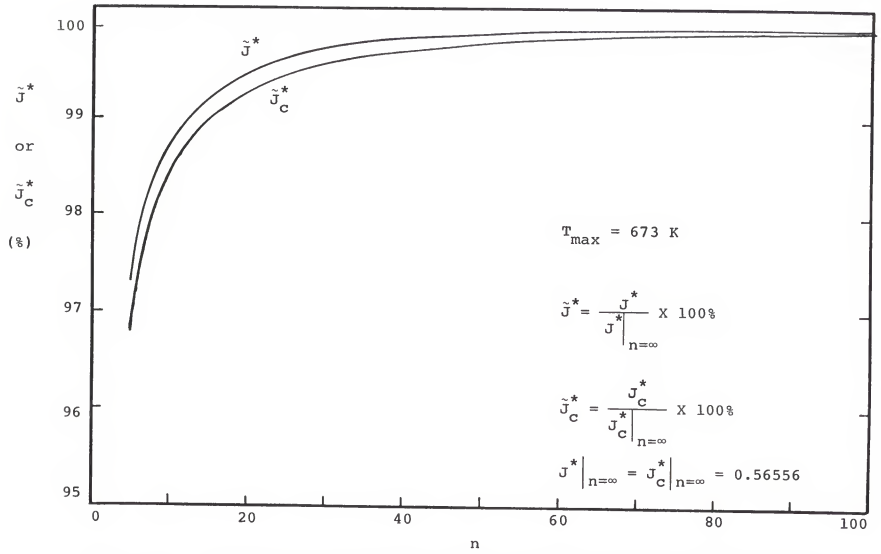

Figure 4-7. Comparison Between Performance Indices Obtained With and Without Constant-Conversion Constraint

enough. In practice, the temperature adjustments are made intermittently because of the slow nature of catalyst deactivation in fixed-beds. From the fact that the curve for $\tilde{J}^*$ lies above the curve for $\tilde{J}_c^*$, it can be concluded that the optimal piecewise control policy is an increasing conversion policy as shown in Fig. 4-2 and 4-4. However, the constant-conversion policy can be used when number of control steps is large, say, 30.

The problem formulation and solution method presented in Section 4-1 is neither restricted to an isothermal reactor nor to a single irreversible reaction. For example, one can consider a reversible reaction taking place in an adiabatic fixed-bed. In this case, the reactor temperatures, T_i's, in Eqs. (4-1) through (4-5) should be replaced by the temperatures at the inlet of the reactor, $(T_{in})_i$'s. Equation (4-2) might then become implicit in X because of the reversible reaction and the nonisothermal reactor. However, X can still be solved numerically. Thus, the problem remains a multivariable optimization problem which can be solved by application of an appropriate numerical method.

CHAPTER 5

OPTIMAL CONTINUOUS CONTROL FOR COMPLEX REACTION

In the experiment described in Section §3-2, we controlled the yield of ethylene oxide at a constant level in a piecewise manner, and verified the feasibility of the feedback control policy presented in Chapter 2.

However, the constant yield policy used is not an optimal policy. It is the purpose of this chapter to obtain an optimal control policy for complex reactions which are parallel with the Langmiur-Hinshelwood rate expressions. We consider here only the optimal continuous control policy since we have shown in the previous chapter that one can use the optimal continuous control policy for piecewise control as long as the number of control steps is large enough.

§5-1 Problem Statement

Consider a parallel reaction network with the Langmiur-Hinshelwood rate expressions for an isothermal fixed-bed such as the ethylene oxidation reaction described in Section §3-2-3. Assume the same active sites are responsible for both reactions, i.e., $h_1 = h_2 = h$ and $\beta = 1$. Equation (3-5) and (3-7) can be rewritten as

$$\frac{dx}{dz} = \frac{\tau h(K_1 + K_2)(1-x)}{1 + K_2(1-x)} \quad ; \quad x\Big|_{z=0}=0 \tag{5-1}$$

and

$$\frac{dx}{dy} = 1 + \frac{K_2}{K_1} \quad ; \quad x\Big|_{y=0} = 0 \tag{5-2}$$

where

$$\tau = WP/F_o,\ K_1 = k_1 k_q,\ K_2 = k_2 k_q,\ \text{and}\ K_q = P_{Ao} k_q$$

The rate of decay of the catalyst activity can be expressed as

$$\frac{dh}{dt} = -K_D h^m \quad ;\quad h\Big|_{z=o} = 1 \tag{5-3}$$

where K_D is the deactivation rate constant. Integrating Eqs. (5-1) and (5-2) from the inlet to the outlet of the reactor yields

$$K_q X - \ln(1-X) = \tau h(K_1 + K_2) \tag{5-4}$$

$$Y = \frac{K_1}{K_1 + K_2} X \tag{5-5}$$

where X and Y are the conversion of ethylene and the yield of ethylene oxide at the outlet of the reactor, respectively.

The optimization problem is to maximize the total amount of yield of ethylene oxide over a fixed total reaction time, t_f, by choosing the optimal temperature-time policy. We assume that the temperature dependence of the rate constants and adsorption equilirbium constant are all of the Arrhennius form:

$$K_i = A_i \exp(-E_i/R_g T) \quad i = 1, 2, q, D \tag{5-6}$$

Since K_D is a strictly monotonic function of temperature, we can use K_D as the control variable to replace T. The constants K_1, K_2 and K_q can be expressed in terms of K_D:

$$K_j = \alpha_j K_D^{P_j} \qquad j = 1,2,q \qquad (5\text{-}7)$$

where $\alpha_j = A_j / A_D^{P_j}$ and $P_j = E_j / E_D$

Thus, our optimization problem is

$$J^* = \max_{K_D(t)} \left\{ \int_0^{t_f} Y dt \right\} = \max_{K_D(t)} \left\{ \int_0^{t_f} \frac{K_1}{K_1 + K_2} X dt \right\} \qquad (5\text{-}8)$$

subject to two local restrictions, Eqs. (5-3) and (5-4). This is a fundamental problem in calculus of variations. The derivation of the necessary conditions for J^* to be maximum is presented in the next section.

§5-2 Necessary Condition

Equation (5-3) indicates that

$$K_D = K_D(h, \dot{h}) \qquad (5\text{-}9)$$

where

$$\dot{h} \equiv \frac{dh}{dt}$$

Since K_1, K_2 and K_q are all functions of K_D, Eqs. (5-4) and (5-5) give

$$Y = Y(K_D, h) = Y(h, \dot{h}) \qquad (5\text{-}10)$$

Thus, the optimization problem of Eq. (5-8) is an elementary problem in the calculus of variations, and the necessary condition for the optimization is an Euler-Lagrange equation (Beveridge and Schechter, 1970):

$$Y - \dot{h}\, Y_{\dot{h}} = C \qquad (5\text{-}11)$$

where

$$Y_{\dot{h}} \equiv \left(\frac{\partial Y}{\partial \dot{h}} \right)_{h,t}$$

and C is an integration constant.

In order to use Eq. (5-11), $\dot{h}Y_{\dot{h}}$ has to be obtained first. Differentiating Eq. (5-7) w.r.t. $\dot{h}$ yields

$$\frac{\partial K_i}{\partial \dot{h}} = \left(\frac{dK_i}{dK_D}\right)\left(\frac{\partial K_D}{\partial \dot{h}}\right) = \left(\frac{p_i K_i}{K_D}\right)\left(-\frac{1}{h^m}\right) \qquad i = 1, 2, q \qquad (5\text{-}12)$$

Multiplying $\dot{h}$ gives

$$\dot{h}\,\frac{\partial K_i}{\partial \dot{h}} = \left(\frac{p_i K_i}{K_D}\right)\left(-\frac{\dot{h}}{h^m}\right) = p_i K_i \qquad (5\text{-}13)$$

Differentiating Eq. (5-4) w.r.t. $\dot{h}$, multiplying $\dot{h}$ and using Eq. (5-13) yields

$$p_q K_q X + K_q(\dot{h}\, X_{\dot{h}}) + \frac{1}{1-X}(\dot{h}\, X_{\dot{h}}) = p_3 \tau (K_1 + K_2)h \qquad (5\text{-}14)$$

where $\quad p_3 = (p_1 K_1 + p_2 K_2)/(K_1 + K_2)$

Rearranging Eq. (5-14) and using Eq. (5-4) for $\tau(K_1 + K_2)h$ we have

$$\dot{h}\, X_{\dot{h}} = \frac{(p_3 - p_q)K_q X - p_3 \ell n(1-X)}{K_q + \frac{1}{1-X}} \qquad (5\text{-}15)$$

Differentiating Eq. (5-5) w.r.t. $\dot{h}$, multiplying $\dot{h}$ and using Eq. (5-13) we obtain

$$\dot{h}\, Y_{\dot{h}} = p_1 \frac{K_1}{K_1 + K_2} X + \frac{K_1}{K_1 + K_2} \dot{h}\, X_{\dot{h}} - p_3 \frac{K_1}{K_1 + K_2} X \tag{5-16}$$

Substituting Eq. (5-16) into (5-11) with the aid of Eq. (5-15) gives

$$\frac{K_1}{K_1 + K_2} \frac{1}{K_q + \frac{1}{1-X}} \left\{ (p_q - p_3) K_q X + p_3 \ell n (1-X) + (K_q + \frac{1}{1-X}) (1 - p_1 + p_3) X \right\} = C \tag{5-17}$$

Equation (5-17) is the necessary condition for J^* to be maximum. The integration constant C can be determined by a boundary condition:

$$h = h_f \quad \text{at} \quad t = t_f \tag{5-18}$$

if h_f is specified, or by a natural boundary condition (Denn, 1969):

$$Y_{\dot{h}} = 0 \quad \text{at} \quad t = t_f \tag{5-19}$$

if h_f is unspecified.

The necessary condition can be simplified if the activation energies for both reactions are equal ($E_1 = E_2$), and the adsorption equilibrium constant K_q is temperature independent ($E_q = 0$). In this case, Eq. (5-17) gives

$$\frac{A_1}{(A_1 + A_2)(A_q + \frac{1}{1-X})} \left\{ -p_1 A_q X + p_1 \ell n (1-X) + (A_q + \frac{1}{1-X}) X \right\} = C \tag{5-20}$$

where A_i is the preexponential factor. Since A_1, A_2, Aq, p_1 and C are all constants, Eq. (5-20) indicates that

$$X = \text{constant} \tag{5-21}$$

In general cases, however, the conversion is not constant. The optimal control policies have to be obtained by numerically solving the necessary condition, Eq. (5-17), along with the local constraints, Eqs. (5-3) and (5-4).

§5-3 Optimal Continuous Control Policies

The predictor-corrector method (Hornbeck, 1975) initiated by fourth order Runge Kutta method was used to solve the ordinary differential Eq. (5-3) while Newton-Raphson iteration (Carnahan et al., 1969) was used for the nonlinear Eqs. (5-4) and (5-17). The kinetic data obtained in Section §3-2-3 and the same parameters used in the experiment were used for obtaining the optimal control policies. Table 5-1 lists these parameters along with the deactivation kinetics used. The boundary condition of Eq. (5-18) was used to obtain the integration constant in Eq. (5-17). This split boundary condition problem was solved by "shooting method" (Hornbeck, 1975). The results are shown in Figs. 5-1 and 5-2.

It can be seen from Fig. 5-1 that the optimal control policy is one of increasing conversion and yield. However, with different deactivation kinetics, the optimal policy becomes one of decreasing conversion and yield, as shown

Table 5-1 Parameters Used for the Optimal Continuous Control Policies

$K_1 = k_1 k_q = 7.028 \times 10^{-2} \exp(-5451/T)$ (mol/s·g-cat·atm)

$K_2 = k_2 k_q = 5.900 \times 10^{-1} \exp(-6632/T)$ (mol/s·g-cat·atm)

$K_q = p_{Ao} k_q = 1.165 \times 10^{-1} \exp(1647/T)$ (-)

$\tau = \frac{WP}{F_o} = 1.134 \times 10^{6}$ (g-cat·atm·s/mol)

$h_f = 0.4$ (-)

$t_f = 1000$ (hr)

$K_D = 4.0 \times 10^{2} \exp(-6000/T)$ (1/hr) in Fig. 5-1

$= 4.0 \times 10^{3} \exp(-7000/T)$ (1/hr) in Fig. 5-2

$p_1 = \frac{E_1}{E_D} = 0.9085$ in Fig. 5-1

$= 0.7787$ in Fig. 5-2

$p_2 = \frac{E_2}{E_D} = 1.105$ in Fig. 5-1

$= 0.9474$ in Fig. 5-2

$m = 1.0$

$E_1/E_2 = 0.822$

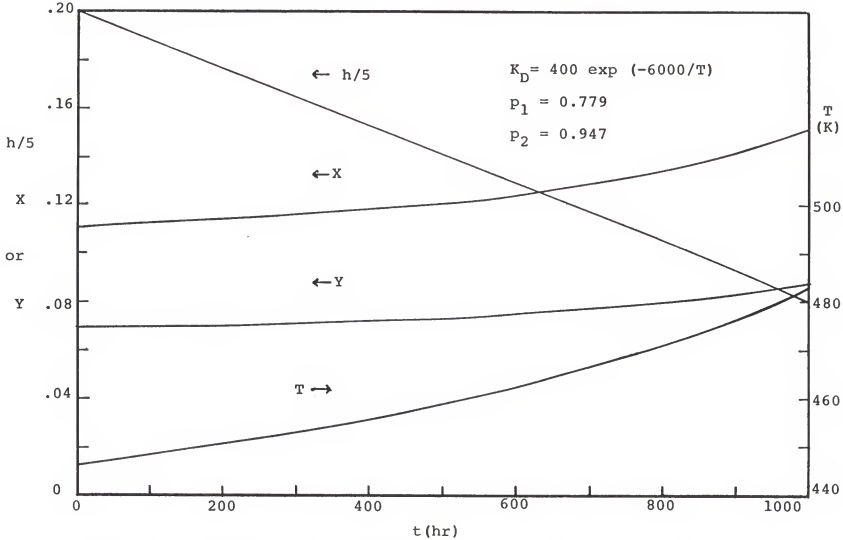

Figure 5-1. Optimal Control Policies for a Parallel Reaction Network with the Langmiur-Hinshelwood Rate Expressions

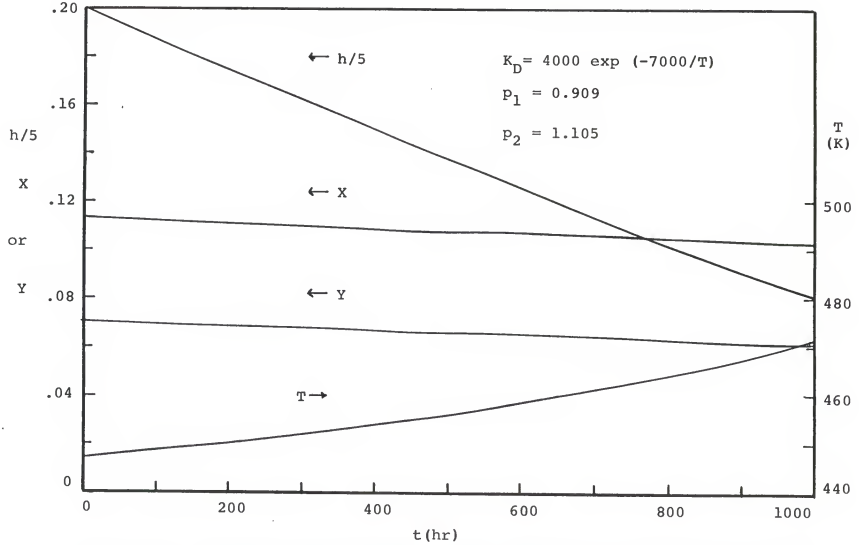

Figure 5-2. Optimal Control Policies for a Parallel Reaction Network with the Langmiur-Hinshelwood Rate Expressions

in Fig. 5-2. This decrease in conversion and yield is due to the large activation energy for deactivation which limits the increase in temperature.

The valuesof the performance index for constant-conversion and constant-yield policies have been calculated for comparison. The results indicate that the control policies shown in Figs. 5-1 and 5-2 are indeed the optimal policies. However, the percent difference between the optimal policy and the constant-conversion policy is less than 0.1% in terms of the performance index. As mentioned earlier, the constant-conversion policy is the optimal policy when $E_1 = E_2$ and $E_q = 0$. For the model reaction studied, E_1 is close to E_2 ($E_1/E_2 = 0.822$) and E_q is small (compared with E_1 and E_2). This explains why the constant-conversion policy is almost as good as the optimal policies shown in Figs. 5-1 and 5-2.

§5-4 Concluding Remarks

We have derived the necessary condition for the optimal continuous control for a parallel reaction network with Langmiur-Hinshelwood rate expressions by direct substitution. The optimal control policies have been obtained by direct numerical integration of Eq. (5-3) with the aid of Eqs. (5-4) and (5-17). Although iterations are required for solving Eqs. (5-4) and (5-17), it takes no more than two iterations for each step in the t-direction because X and K_D are smooth functions of t and the values in the previous step provide very good initial guesses for the current step. In fact, it

took less than 3 seconds CPU time of IBM 360/370 computer to generate all the data shown in Fig. 5-1, including 5 iterations for shooting the boundary condition, $h = h_f$ at $t = t_f$. This efficiency can never be achieved if the Pontryagin maximum principle (Pontryagin et al., 1962) and the Hamiltonian are used (Ogunye and Ray, 1971).

CHAPTER 6

OPTIMAL CONTROL AND DESIGN

We address in this chapter the problem of how a fixed-bed with catalyst deactivation should be designed to obtain the best possible performance when it is controlled optimally. In particular, we ask what the size of the reactor should be that maximizes a certain performance index when the temperature is also manipulated to maximize the performance index. This is a design practice in which process control is taken into consideration. In order to clearly demonstrate the interrelationship between design and control and the advantage that can be gained by utilizing this interrelationship, we assume for the time being that the detailed knowledge of deactivation is available.

§6-1 An Optimization Problem of Piecewise Control and Design

Consider an optimization problem of a single irreversible reaction taking place in an adiabatic reactor given by

$$J^* = \max_{\tau,\ T_{in}(t)} \qquad J = \max_{\tau,\ T_{in}(t)} \frac{1}{\tau t_f} \int_0^{t_f} X dt \tag{6-1}$$

subject to the system equations of Eqs. (2-1) and (2-2) with $(mC_p)_c = 0$ for the adiabatic reactor under consideration

and subject to $T_{in} \leq (T_{in})_{max}$ with a fixed t_f. The problem is to maximize the performance index J, which is the conversion (X) integrated over the catalyst life t_f per unit reactor volume and unit on-stream time, by properly choosing τ and $T_{in}(t)$. This two-parameter optimization problem can be solved one at a time by first searching for the maximum for a given τ and then finding the value of τ that yields the maximum. For a fixed τ, it is a Bolza's problem (Bliss, 1961) and the extremum condition obtained by Chou et al. (1967) and Ogunye and Ray (1971) is to maintain the conversion at a constant level until the maximum allowed temperature is reached and then to remain at the maximum if only one rate constant is involved. For the deactivation problem under consideration the policy is not directly applicable since the rate constant cannot be separated out. However, the constant conversion policy is still a suboptimum which is often used in practical operation of chemical plants. Thus, we apply the constant conversion policy for the problem considered. Since the feedback control policy obtained earlier is for maintaining a constant conversion level, the problem is simply that of finding an initial value of T_{in} (or the desired conversion level) if we use the control policy, for T_{in} can be set at $(T_{in})_{max}$ once $(T_{in})_{max}$ is reached.

The optimization problem was solved for the reaction system in Tables 3-1 and 3-2 using the control algorithms of Eqs. (2-16) through (2-18) with the constraints of $t_f = 10^5$ sec. and $(T_{in})_{max} = 720$ K. The typical behavior of $T_{in}(t)$ and the outlet conversion is shown in Fig. 6-1 for the bandwidth ΔX of 5% and the initial inlet temperature of 691 K (or conversion of 87.2%). In accordance with the constraint on t_f and the extremum condition, T_{in} stays at the maximum allowed temperature once it reaches the maximum and the conversion decreases with time, eventually reaching a conversion of 54.5% at $t = t_f$, at which time the catalyst is regenerated. As indicated earlier, the optimization problem for a chosen τ is that of finding an initial conversion (or initial inlet temperature) that yields a maximum. The solutions obtained for various τ are shown in Fig. 6-2 for a bandwidth of 0.05. A few observations can be made from the figure. The results show that for a given τ, the extremum condition does yield a maximum. Furthermore, the value of the performance index is much more sensitive to a choice of the initial inlet temperature (or the initial conversion) at relatively lower values of the inlet temperature than at higher values. The locus of the maximum values of J for various τ is given in Fig. 6-2 as the dotted line. As apparent from the figure, there exists a maximum at around $\tau = 22$ sec. The performance index normalized with respect to the index corresponding

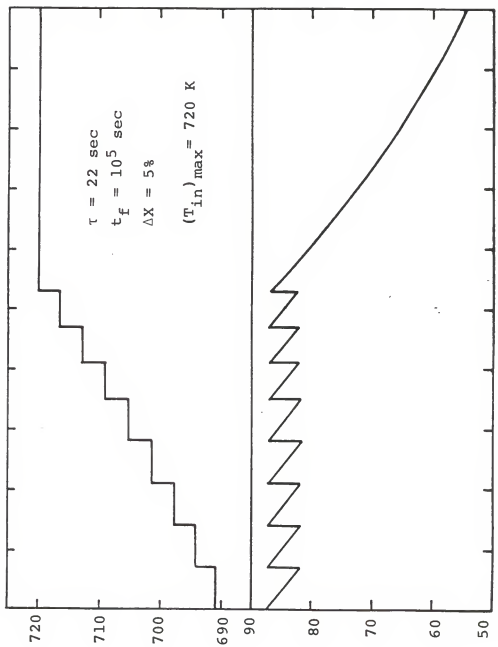

Figure 6-1. Inlet Temperature and Conversion Behavior for an Optimal Control with Bandwidth of 0.05

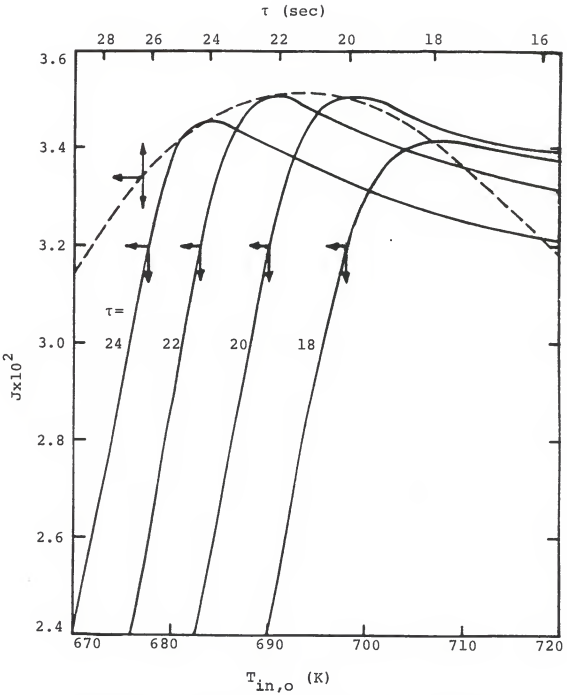

Figure 6-2. Performance Index as a Function of Reactor Size and Initial Inlet Temperature. The dotted line shows the locus of J^*.

to $\tau = 22$ sec., when the reactor is operated optimally, is shown in Fig. 6-3 as a function of the reactor size τ. It is seen that the performance index [Eq. (6-1)] doubles (τ of 8 sec. vs. τ of 22 sec.) when the reactor is sized optimally. This result confirms the intuitive reasoning that the best possible reactor performance obtainable by process control is inherently dictated by process design. It also confirms the fact that a significant improvement can be made by combining process design with process control.

§6-2 An Optimization Problem of Continuous Control and Design

In this section, we give an example of design practice in which the optimal continuous control is taken into consideration. Here we consider an isothermal fixed-bed where a first order reaction subject to first order deactivation takes place. The system equations are the same as those in Table 4-1, but the temperature is controlled continuously. The performance index is given by

$$J^* = \max_{\tau, T(t)} J = \max_{\tau, T(t)} \frac{1}{\tau t_f} \left[\int_0^{t_f} X dt - \mu \right] \tag{6-2}$$

where μ is the cost incurred due to the reactor shut-down for regenerating or replacing the spent catalyst. The constant conversion policy which is indeed the optimal

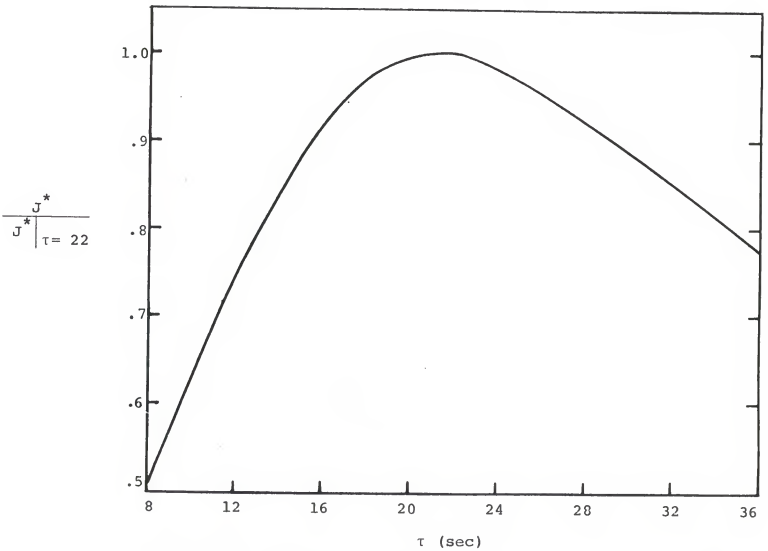

Figure 6-3. Maximum Values of Performance Index for Various Reactor Sizes

control policy for this reaction system (Crowe, 1970) was applied to solve the optimization problem of Eq. (6-2) with the following rate constants and restrictions

$$k_D = 1.0 \times 10^4 \exp(-8000/T) \qquad (1/hr)$$

$$k_1 = 1.0 \times 10^6 \exp(-10000/T) \qquad (1/S)$$

$$473\ K \leq T \leq 673\ K$$

$$t_f = 2000\ (hr)$$

$$\mu = 220\ (hr)$$

The solutions obtained are plotted in Fig. 6-4. The behavior of the performance index is similar to that shown in Fig. 6-2, i.e. for a given reactor size (τ), J depends on the initial temperature chosen (T_o) and does yield a maximum. The locus of the maximum value of J for various of τ is shown in Fig. 6-4 as the dotted line. Again, we can see from the figure there exists an optimal reactor size, i.e. τ = 13 sec. Further observations of the figure indicate that a reactor of τ = 15 second gives better performance than a reactor of τ = 10 second does if both are controlled optimally (T_o = 595.9 K for τ = 15 sec. and T_o = 605.4K for τ = 10 sec). However, the latter performs better than the former does if same initial temperatures are chosen, say, 620 K. This indicates that both the deactivation of catalyst and the corresponding process control should be considered during the design phase to choose an optimal reactor size.

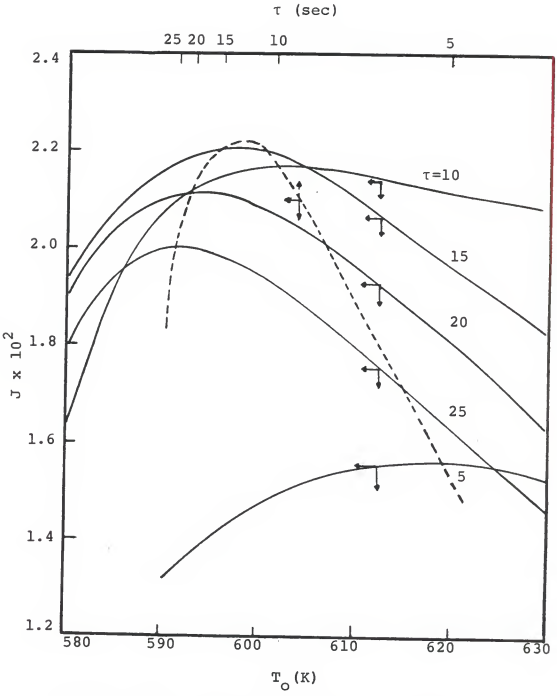

Figure 6-4. Performance Index as a Function of Reactor Size and Initial Temperature. The dotted line shows the locus of J^*.

The normalized optimal performance index is plotted in Fig. 6-5 as a function of reactor size. It can be seen from the figure that the performance index can be improved significantly if the optimal size is chosen.

§6-3 Concluding Remarks

We have so far assumed that detailed knowledge of catalyst deactivation is available. The same optimal control and design can still be carried out if some knowledge of deactivation is available, however uncertain it may be, since what is sought in such a case would be approximate values of the optimal size and inlet temperature and some directions as to what to choose. In the example considered in Section §6-1, for example, one would choose a relatively high initial conversion (or a high inlet temperature) rather than a low initial conversion in view of the sensitivity discussed earlier.

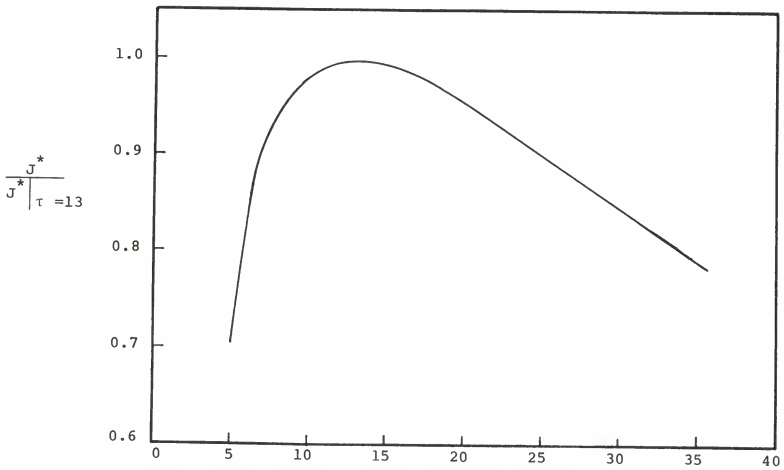

Figure 6-5. Maximum Values of Performance Index for Various Reactor Sizes

CHAPTER 7

CONCLUSIONS

A measure of the extent of deactivation can be determined from the on-line measurements of inlet temperature and outlet concentration along with the intrinsic rate of a single reaction for an isothermal or an adiabatic fixed-bed reactor. Additional measurements of coolant temperature are required for a nonadiabatic fixed-bed reactor. These results can be extended to multiple reactions in a rather straightforward manner. The measure of deactivation is determined in such a way that a piecewise feedback control scheme follows directly from it. This feedback control maintains the conversion within a band about a desired level of conversion. These results enable one to carry out feedback control of the reactor in any desired manner without any knowledge of catalyst deactivation. Further, the results are applicable to any type of deactivation; whether the deactivation is dependent or independent of reactant concentration and whether the deactivation kinetics are separable or nonseparable from main reaction kinetics.

The feedback control policy considered is a piecewise rather than continuous control. The piecewise control necessitated by the pseudo steady-state nature of deactivation

with respect to the reactor response time allows us to avoid one problem in any feedback control involving dead time due to sampling and another one associated with reactor transients. Inherent in the pseudo steady-state assumption is the fact that the rate of deactivation is much slower than the rate of reaction. In terms of time, the deactivation is of the order of months for the majority of reactions carried out in a fixed bed whereas the transients reach the steady state in a few residence-times which is of the order of seconds. Therefore, the problem associated with "wrong way" transients [e.g., Crider and Foss (1966)] can be avoided since by the time a control action is taken, the reactor reaches a new, stable steady state. Further, the effect of dead time, which is of the order of minutes, on deactivation can be neglected since the extent of deactivation changes little in minutes.

The feedback control policy has been applied to a simulated adiabatic reactor where a single reaction affected by diffusion and poisoning take place, and to a laboratory isothermal reactor where ethylene oxidation reactions affected by sintering take place. The results show that one can indeed control the conversion or yield in any desired manner without any a priori knowledge of the deactivation kinetics, and that the aforementioned problems of wrong way transients and dead time do not occur during normal operation.

The problem of finding the optimal piecewise control policy can be formulated as a multivariable optimization problem. For a single irreversible reaction affected by independent deactivation, the optimal piecewise control policy is one of increasing conversion. However, the well-known constant conversion policy used in the continuous control system can be applied to the piecewise control system with little loss in reactor performance if the number of piecewise control actions is large. The solution method developed is applicable to any reaction taking place in any reactor.

The necessary condition for optimal control in complex reaction systems (such as ethylene oxidation reactions) can be derived by direct substitution. The optimal control policy is either an increasing conversion policy or a decreasing conversion policy, depending upon the ratio of activation energy of the main reaction to that of the deactivation reaction. The direct substitution method is shown to be more efficient than the commonly used method that relies on the Pontryagin's minimum principle through a Hamiltonian formulation.

The problem of combining process control with process design, with due consideration of catalyst deactivation for both, can be solved in a straightforward manner using the feedback control scheme and the approach of reactor point effectiveness.

However, detailed knowledge of deactivation has to be known to solve this problem. It is shown that the choice of reactor size can substantially affect the reactor performance. The solution yields the optimal reactor size and an optimal way of manipulating the inlet temperature based on on-line measurements for those reactors for which detailed knowledge of deactivation is available. Even when there is some uncertainty about the knowledge, the procedure yields approximate ranges of the optimal values and also some directions as to what is to be chosen. These results enable one to fully account for catalyst deactivation for a substantial improvement in the reactor performance.

REFERENCES

Akella, L.M., "Reactor Design and Analysis for Exothermic Reactions and Characterization of Ethylene Oxidation Reactions," Ph.D. Dissertation, University of Florida (1983).

Beveridge, G., and R.S. Schechter, Optimization: Theory and Practice, McGraw-Hill, New York (1970).

Bliss, G.A., Lectures on the Calculus of Variations, The University of Chicago Press, Chicago (1961).

Box, M.J., "A Comparison of Several Current Optimization Methods, and the Use of Transformations in Constrained Problems," Computer Journal 9, 67 (1966).

Carnahan, B., H.A. Luther, and J.O. Wilkes, Applied Numerical Methods, Wiley, New York (1969).

Chou, A., W.H. Ray, and R. Aris, "Simple Control Policies for Reactors with Catalyst Decay," Trans. Instn. Chem. Engrs., 45, T153 (1967).

Crider, J.E., and A.S. Foss, "Computational Studies of Transients in Packed Tubular Chemical Reactors," AIChE J., 12, 514 (1966).

Crowe, C.M., "Optimization of Reactors with Catalyst Decay: I. Single Tubular Reactor with Uniform Temperature," Can. J. Chem. Eng., 48, 576 (1970).

Denn, M.M., Optimization by Variational Methods, McGraw-Hill, New York (1969).

Dettwiler, H.R., A. Baiker, and W. Richarz, "Kinetics of Ethylene Oxidation on a Supported Silver Catalyst," Helvetica Chimica Acta, 62, 1689 (1979).

Haas, W.R., L.L. Tavlarides, and W.J. Wnek, "Optimal Temperature Policy for Reversible Reactions with Deactivation: Applied to Enzyme Reactors," AIChE J., 20, 707 (1974).

Hornbeck, R.W., Numerical Methods, Quantum Publishers, New York (1975).

Kovarik, F.S., and J.B. Butt, "Reactor Optimization in the Presence of Catalyst Decay," Cat. Rev., 24, 449 (1982).

Lee, H.H., "Catalyst Sintering and Pellet Effectiveness," Chem. Eng. Sci., 36, 950 (1981).

Lee, H.H., and J.B. Butt, "Heterogeneous Catalytic Reactors Undergoing Chemical Deactivation, Part I: Deactivation Kinetics and Pellet Effectiveness," AIChE J., 28, 405 (1982a).

Lee, H.H., and J.B. Butt, "Heterogeneous Catalytic Reactors Undergoing Chemical Deactivation, Part II: Design and Analysis: Approach of Reactor Point Effectiveness," AIChE J., 28, 410 (1982b).

Lee, H.H., and E. Ruckenstein, "Catalyst Sintering and Reactor Design," Cat. Rev., 25, 475 (1983).

Lee, S.I., and C.M. Crowe, "Optimal Temperature Policies for Batch Reactors with Decaying Catalyst," Chem. Eng. Sci., 25, 743 (1970).

Levenspiel, O., and A. Sadana, "The Optimal Temperature Policy for a Deactivating Packed-Bed Reactor," Chem. Eng. Sci., 33, 1393 (1978).

Ogunye, A.F., and W.H. Ray, "Optimal Control Policies for Tubular Reactors Experiencing Catalyst Decay," AIChE J., 17, 43 (1971).

Pommersheim, J.M., L.L. Tavlarides, and S. Mukkavilli, "Restrictions and Equivalence of Optimal Temperature Policies for Reactors with Decaying Catalysts," AIChE J., 26, 327 (1980).

Pontryagin, L.S., V.G. Boltyznskii, R.V. Gamkrelidze, and E.F. Mishchenko, The Mathematical Theory of Optimal Processes, Interscience Publishers, New York (1962).

Spath, H.T., and K.D. Handel, "Kinetics and Mechanism of the Oxidation of Ethylene over Silver Catalysts," Adv. Chem. Ser. Chem. React. Eng. II, 133, 395 (1974).

Szepe, S., and O. Levenspiel, "Optimal Temperature Policies for Reactors Subject to Catalyst Deactivation--I. Batch Reactor," Chem. Eng. Sci., 23, 881 (1968).

Wheeler, A., "Reaction Rates and Selectivity in Catalyst Pores," Adv. in Cat., 2, 249 (1955).

BIOGRAPHICAL SKETCH

The author was born on January 9, 1955, in Taipei, Taiwan, Republic of China. He received his B.S. degree in chemical engineering from National Taiwan University, Taipei, Taiwan, in 1977. After serving as a Second Lieutenant in the Chinese ROTC for two years, he came to the United States for graduate studies. The author received his M.S. degree in chemical engineering from West Virginia University, Morgantown, West Virginia, in 1981 and has attended the Department of Chemical Engineering, University of Florida, for Ph.D. study since then. His career interest is teaching and research in catalytic reactor design and in manufacturing semiconductor crystals.

I certify that I have read this study and that in my opinion it conforms to acceptable standards of scholarly presentation and is fully adequate, in scope and quality, as a dissertation for the degree of Doctor of Philosophy.

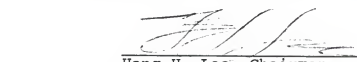

Hong H. Lee, Chairman
Associate Professor of
Chemical Engineering

I certify that I have read this study and that in my opinion it conforms to acceptable standards of scholarly presentation and is fully adequate, in scope and quality, as a dissertation for the degree of Doctor of Philosophy.

Gar B. Hoflund
Associate Professor of
Chemical Engineering

I certify that I have read this study and that in my opinion it conforms to acceptable standards of scholarly presentation and is fully adequate, in scope and quality, as a dissertation for the degree of Doctor of Philosophy.

Chen-Chi Hsu
Professor of Engineering
Sciences

I certify that I have read this study and that in my opinion it conforms to acceptable standards of scholarly presentation and is fully adequate, in scope and quality, as a dissertation for the degree of Doctor of Philosophy.

John P. O'Connell
Professor of Chemical
Engineering

I certify that I have read this study and that in my opinion it conforms to acceptable standards of scholarly presentation and is fully adequate, in scope and quality, as a dissertation for the degree of Doctor of Philosophy.

Spyros A. Svoronos

Spyros Svoronos
Assistant Professor of
Chemical Engineering

This dissertation was submitted to the Graduate Faculty of the College of Engineering and to the Graduate Council, and was accepted as partial fulfillment of the requirements for the degree of Doctor of Philosophy.

Hubert A. Beers

Dean, College of Engineering

Dean for Graduate Studies
and Research